EXPERIMENTAL RESULTS FOR VISCOSITY MEASUREMENTS PERFORMED ON THE INTERNATIONAL SPACE STATION USING DROP COALESCENCE IN MICROGRAVITY

A Thesis

Presented for the

Masters of Science Degree

The University of Tennessee

Brian Michael Godfrey

August 2011

In Memory of
Paul Austin Higdon
1913-2006

ACKNOWLEDGMENTS

I would like to thank my advisor Dr Basil Antar, for all his help and advice on this project. I would also like to thank Dr. Trevor Moeller and Dr. Alfonso Pujol, Jr. for their help and advice as members of my committee. Most of all I would like to thank my friends and family for their support, and encouragement throughout my life.

ABSTRACT

Current commonly use viscosity measurement techniques cannot be used for all types of fluids. For fluids in the under cooled region a new method of measuring the viscosity is required. A process of viscosity measurement, by measuring the speed of droplet coalescence in a microgravity environment, was developed. This paper analyses validation experiments performed on the International Space Station. Four experiments were analyzed. Two of the experiments provided results consistent with the known value for the viscosity. One of the experiments did not provide sufficient data for analysis. The final experiment had possible errors due to the experimental setup. The resulting data from these experiments demonstrated that the method is feasible. However, more experiments are needed to fully verify the process.

TABLE OF CONTENTS

ACKNOWLEDGMENTS iii

ABSTRACT iv

LIST OF FIGURES vii

LIST OF TABLES x

INTRODUCTION 1

MATHEMATICAL MODEL 8

Conservation Equations 8

2-D Analysis 9

Axis-Symmetric Geometry 12

NUMERICAL SOLUTION 14

Methodology 15

Computer Programs 16

Surface Geometry Generator 16

Double Symmetry Simulator 17

Single Symmetry Simulator 19

EXPERIMENTAL SET UP 21

KC-135 Tests 21

ISS Tests 22
ANALYSIS 25
Automated Analysis Difficulties 25
Acquiring Data 27
Preparing Videos 27
Measuring Contact Diameter 27
Analyzing the Data 30
RESULTS AND CONCLUSIONS 33
Individual details 34
Sample B1-1 34
Sample B1-2 38
Sample B1-3 43
Sample B1-4 44
Discussion 48
RECOMMENDATIONS FOR FUTURE WORK 50
BIBLIOGRAPHY 53
VITA 56

LIST OF FIGURES

Figure 1: Couette Flow Between Two Plates (White) 1

Figure 2: Falling Sphere Viscometer 4

Figure 3: Rotating Cylinder Viscometer using Falling Mass to Generate a constant force 5

Figure 4: Surface Point Generator Point Location, for Single Symmetry Case ... 17

Figure 5: Points for Double Symmetry Case (Lehman) 18

Figure 6: Theoretical Curve for Double Symmetry 18

Figure 7: Progression of Two Equal Drops over Time (Antar, Ethridge and Maxwell) 19

Figure 8: Progression of Two Unequal Drops over Time (Antar, Ethridge and Maxwell) 20

Figure 9: KC135 Experimental Setup (Lehman) 21

Figure 10: Photo of Experiment Being Carried Out on the KC135 22

Figure 11: ISS Experimental Setup 23

Figure 12: Experiment Being Carried Out on ISS 24

Figure 13: Inconsistencies in Background Color and Intensity 26

Figure 14: Glair and Support Strings Causing Difficulties in Locating Contact Points 26

Figure 15: Graphical Interface for Selecting Points for Contact Radius 28

Figure 16: Scale Photo for Determining Length Scale for Photos 28

Figure 17: Location of Contact Points for Calculating Contact Radius 29

Figure 18: Resulting Experimental Data 29
Figure 19: Graphical Interface for Determining Viscosity 31
Figure 20: Effects of Changing the Time Constant t_0 on the Theoretical Data .. 32
Figure 21: Effects of Changing the Viscosity on the Theoretical Data 32
Figure 22: Sample B1-1 34
Figure 23: Sample B1-1 Overall Data Fit 35
Figure 24: Sample B1-1 Initial Data Fit 35
Figure 25: Sample B1-1 Final Data Fit 36
Figure 26: Combined Graph of Measurements for Sample B1-1 36
Figure 27: Sample B1-1 with Theoretical Curve for Known Viscosity 37
Figure 28: Image of Strings Holding Droplets Apart and Effecting Viscosity Measurements 38
Figure 29: Sample B1-2 38
Figure 30: Sample B1-2 Overall Data Fit 39
Figure 31: Sample B1-2 Initial Data Fit 40
Figure 32: Sample B1-2 Final Data Fit 40
Figure 33: Combined Graph of Measurements for Sample B1-2 41
Figure 34: Sample B1-2 with Theoretical Curve for Known Viscosity 42
Figure 35: Sample B1-3 43
Figure 36: sample B1-3 showing overlap of Droplets During Initial Coalescence 43
Figure 37: Sample B1-3 Final Data Fit 44

Figure 38: Sample B1-4 44
Figure 39: Sample B1-4 Overall Data Fit 45
Figure 40: Sample B1-4 Initial Data Fit 46
Figure 41: Sample B1-4 Final Data Fit 46
Figure 42: Combined Graph of Measurements for Sample B1-4 47
Figure 43: Sample B1-4 with Theoretical Curve for Known Viscosity 48
Figure 44: Glair and Support Strings Causing Difficulties in Isolating Drops for Automatic Analysis 50
Figure 45: Possible Background Grids for Future Experiments 52

LIST OF TABLES

Table 1: List of Fluid Properties for Experiments on the KC135 and ISS 25

Table 2: Viscosity Results For all Samples..... 33

INTRODUCTION

Viscosity of a fluid is defined as a quantitative measure of a fluid's resistance to flow (White, 2003). More specifically, it determines the fluid strain rate that is generated by a given applied shear stress. Plane Couette flow is a simple fluid flow example that demonstrates the effects of viscosity. Couette flow describes the behavior of a fluid between two plates where one plate is stationary and the other has a constant force applied to it. The velocity of the top plate is determined by the viscosity of the fluid. The more viscous the fluid the slower the plate will move.

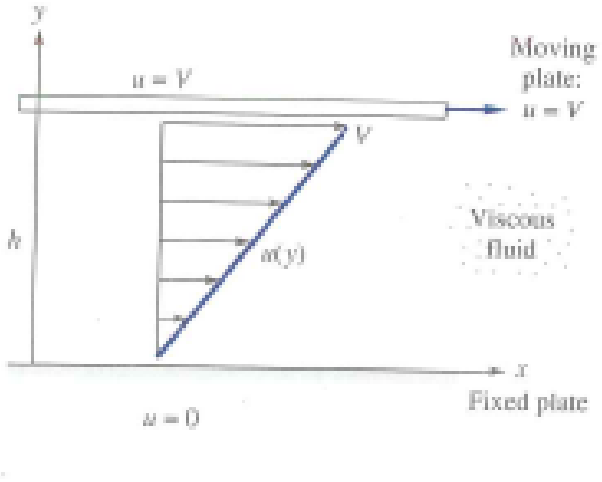


Figure 1: Couette Flow Between Two Plates (White, 2003)

Viscosity is generally measured as a force time per length squared ($\frac{F\,t}{L^2}$). In the International System of Units (SI) the units of measure, viscosity is in Newton seconds per meter squared ($\frac{Ns}{m^2}$) which is also equal to a Pascal second ($Pa\ s$). In the Imperial units viscosity is measured in pounds-force second per foot squared ($\frac{lbf\ s}{ft^2}$). For the

sake of this report all measurements will be in SI units of Newton, meter, and second (N- m-s).

Viscosity is a thermodynamic variable varying as a function of pressure and temperature. Generally speaking the viscosity of a fluid increases only weakly with pressure (White, 2003). Temperature can have a major effect on the value of the viscosity of a fluid. In gasses, viscosity increases with temperature, due to the increased interaction between gas molecules. In liquids, the viscosity decreases with the increase in temperature, due to the increased spacing between molecules.

Current viscosity measurement techniques are not viable for all types of fluids. One such type of fluid is known as under cooled fluids. An under cooled fluid is a liquid or gas that has been cooled below its freezing or sublimation point without undergoing transition to a solid state. When an under cooled fluid, such as glass at high temperatures, comes into contact with a foreign substance it goes through a phase shift and instantly begins to go through the glass transition before a viscosity measurement can be made (Novikov & Sokolov, 2004). Since the viscosity cannot be determined the viscosity is commonly extrapolated from known values in the non-under cooled region shown in Figure 2. The viscosities of glass in this region can be helpful in the manufacturing of fiber optic cables.

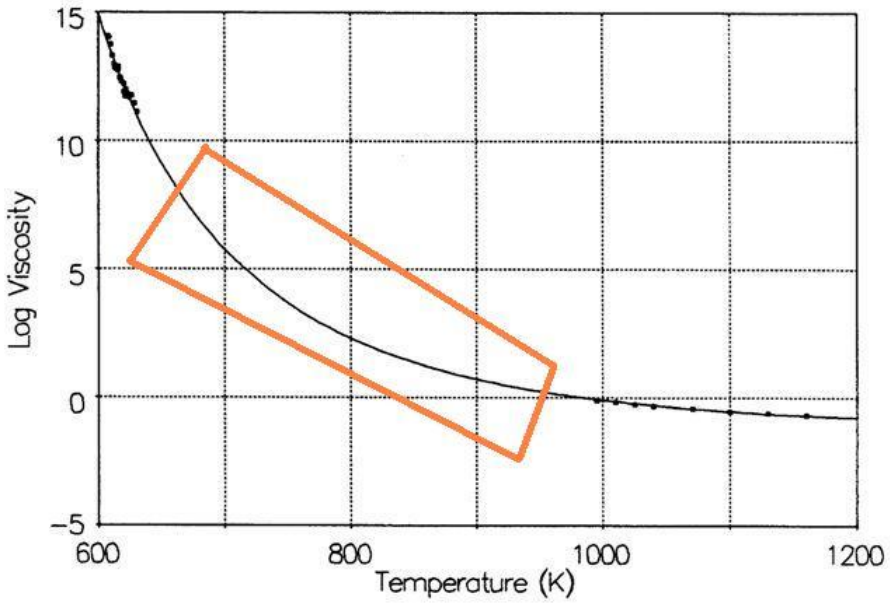


Figure 2: Plot Showing the Unknown Region of the Glass Viscosity Curve

Current commonly used viscosity measurement techniques require that the fluid comes into contact with a solid material. One of these common viscosity measurement techniques is the falling sphere viscometer shown in Figure 3 (Sutterby, 1973). The fluid is stationary in a tube and a sphere of known diameter and density is dropped into the tube. If the density of the fluid is known the viscosity can be determined from the terminal velocity of the sphere by using stokes law. In the example in Figure 3 the velocity is measured by timing how long it takes the sphere to pass between the two lines. Multiple spheres of different diameters and densities can be used to improve accuracy.

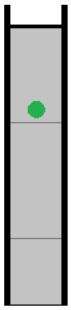


Figure 3: Falling Sphere Viscometer

Another method of measuring the viscosity of a fluid is the rotating viscometer (Figure 4). The rotating viscometer is a cylinder within a cylinder where the gap between the cylinders, filled with fluid, is known and one of the cylinders is rotated with a known force (Dontula, Macosko, & Scriven, 2005). Using the equations for Couette flow the viscosity can be determined from the velocity of the rotating cylinder. Both of these viscometers require a foreign element to come in contact with the fluid. This cannot be done with under cooled fluids so another method must be found.

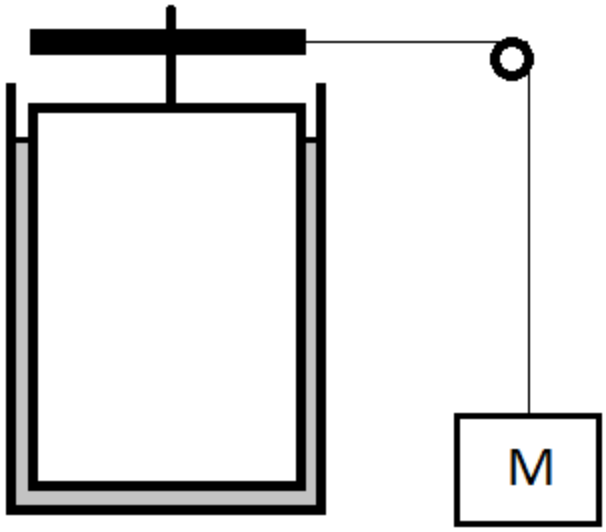


Figure 4: Rotating Cylinder Viscometer using Falling Mass to Generate a constant force

The method described in this thesis was devised by Antar (Antar, Ethridge, & Maxwell, 2003) in order to eliminate the problems of measuring the viscosity of under cooled liquids. This method involves the study of how droplets coalesce within a micro gravity environment. Using a micro gravity environment allows for the simplification of the equations of fluid motion in order to allow them to be solvable. A microgravity environment is produced by creating a dynamic weightless environment, or the apparent lack of gravity that occurs in all freefalling objects (Antar & Nuotio-Antar, 1993). Several ways to produce a micro gravity environment include drop towers, sounding rockets, parabolic flight, and orbiting spacecraft. Each of these methods has a different time length at which a micro gravity environment can be achieved (Figure 5). A drop tower is on the order of a few seconds. A sounding rocket produces around 4 to 15 minutes of microgravity (Antar & Nuotio-Antar, 1993); however the processes would have to be entirely automated. For these experiments the time scales are too

short for proper measurements to be taken. Therefore, initial experiments were run on NASA's KC135 weightless wonder, and the subsequent experiments that were analyzed in this paper were run on the International Space Station (ISS).

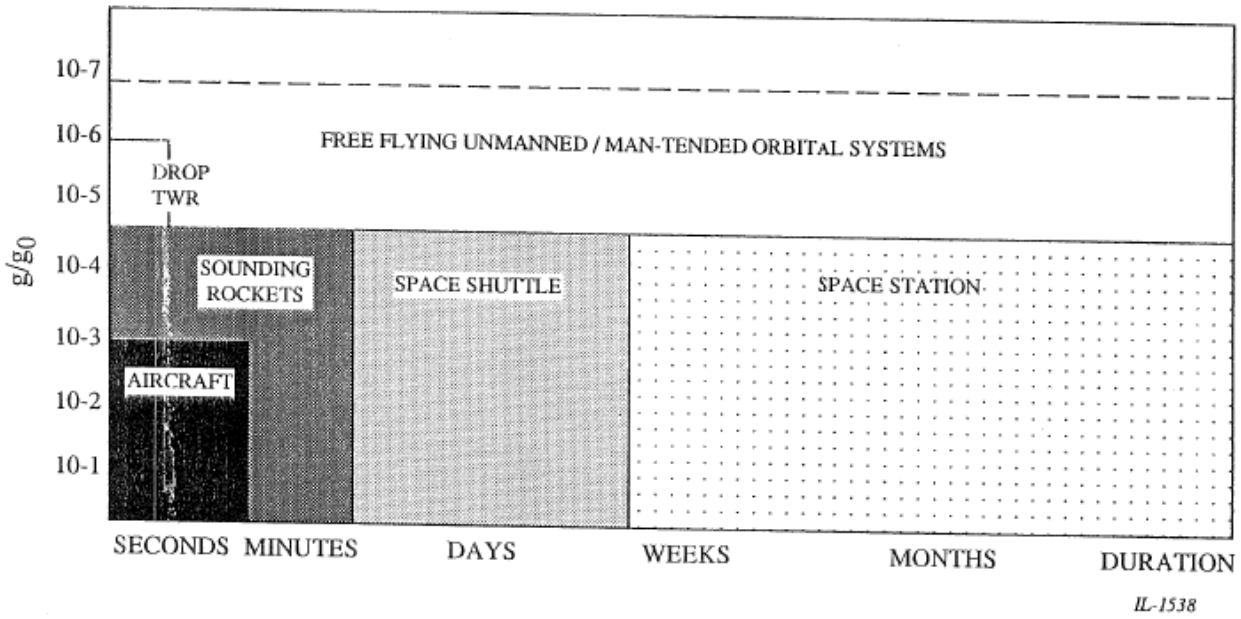


Figure 5: Chart showing the methods of producing microgravity and duration of microgravity state (Antar & Nuotio-Antar, 1993)

Experiments were performed on NASA's KC-135 in order to validate the experiments. These experiments involved bringing 2 droplets sitting on the tips of syringe needles together and allowing them to coalesce. Experiments performed on the KC-135 experienced a lot of g-jitter. The experiment had to be designed so that it can be set up and run in the 20 seconds of microgravity the KC-135 provides each cycle. Therefore, the setup introduced several sources of error into the calculations. An experimental setup for use on the ISS was devised in order to take advantage of the unlimited setup time and test length that the station can provide. These experiments

were filmed and the videos are analyzed to determine the viscosity. The purpose of this thesis is to validate the utility of this technique by comparing the experimentally measured viscosity with the accepted viscosity value of the test fluid.

MATHEMATICAL MODEL

Conservation Equations

The mathematical model for the coalescence of the droplets was derived in (Antar, Ethridge, & Maxwell, 2003). The droplet coalescence is described by the equations of motion for incompressible fluid flow. The analysis starts with the conservation equations for mass and momentum:

$$\vec{\nabla}\cdot \mathbf{u} = 0 \tag{1}$$

$$\frac{\partial \mathbf{u}}{\partial \mathrm{t}} + \mathbf{u}\cdot\vec{\nabla}\,\mathbf{u} = -\frac{1}{\rho}\vec{\nabla}\,\mathrm{p} + \nu\vec{\nabla}^2\mathbf{u} \tag{2}$$

where $\boldsymbol{u} = (u_1, u_2, u_3)$, is the velocity vector field of the fluid, p is the fluid pressure field, ρ is the density of the fluid, and ν is the fluid kinematic viscosity. Since the flow for this analysis is concerned with slow moving capillary motion the inertia terms can be ignored, leaving the equation

$$\rho\frac{\partial \boldsymbol{u}}{\partial t} + \mu\vec{\nabla}^2\boldsymbol{u} - \vec{\nabla}\,p = 0 \tag{3}$$

where μ is the fluid dynamic viscosity($\mu = \rho\nu$). The resulting conservation equations are linear partial differential equations describing the viscous flow for slow moving non-accelerating flows such as the coalescence of two droplets. The system of equations is linear; therefore, there exists a closed form analytical solution for this system in terms of the Stokeslets (Happel, 1965). Since we are looking at the free surface movement as the droplets coalesce, the process is primarily a capillary one. Therefore the

solutions to the conservation equations must satisfy the free surface boundary condition (Antar, Ethridge, & Maxwell, 2003) given by the equation:

$$\boldsymbol{\Gamma} \cdot \boldsymbol{n} = -\sigma \left(\frac{1}{R_1} + \frac{1}{R_2} \right) \boldsymbol{n} = b \tag{4}$$

where $\boldsymbol{n}$ is the unit normal at the free surface in the direction away from the fluid, σ is the coefficient of surface tension, R_1 and R_2 are the principal radii of the curvature of the free surface, and $\boldsymbol{\Gamma}$ is the stress tensor given in Cartesian coordinates as:

$$\boldsymbol{\Gamma}_{\mathrm{ij}} = -\mathrm{p}\delta_{\mathrm{ij}} + 2\mu\varepsilon_{\mathrm{ij}} \tag{5}$$

$$\varepsilon_{\mathrm{ij}} = \frac{1}{2}\left(\frac{\partial u_i}{\partial x_j} + \frac{\partial u_j}{\partial x_i} \right) \tag{6}$$

Where δ_{ij}, is the Kronecker Delta. For the analysis of the droplet coalescence the stress tensor will be given in cylindrical or spherical coordinates. However for demonstration of the calculations we will use 2-D Cartesian coordinates and then move to a 3-D analysis.

2-D Analysis

For the two dimensional case, Figure 6, the conservation equations and the boundary conditions, equations (1), (3) and (4) take the following form (Antar, Ethridge, & Maxwell, 2003):

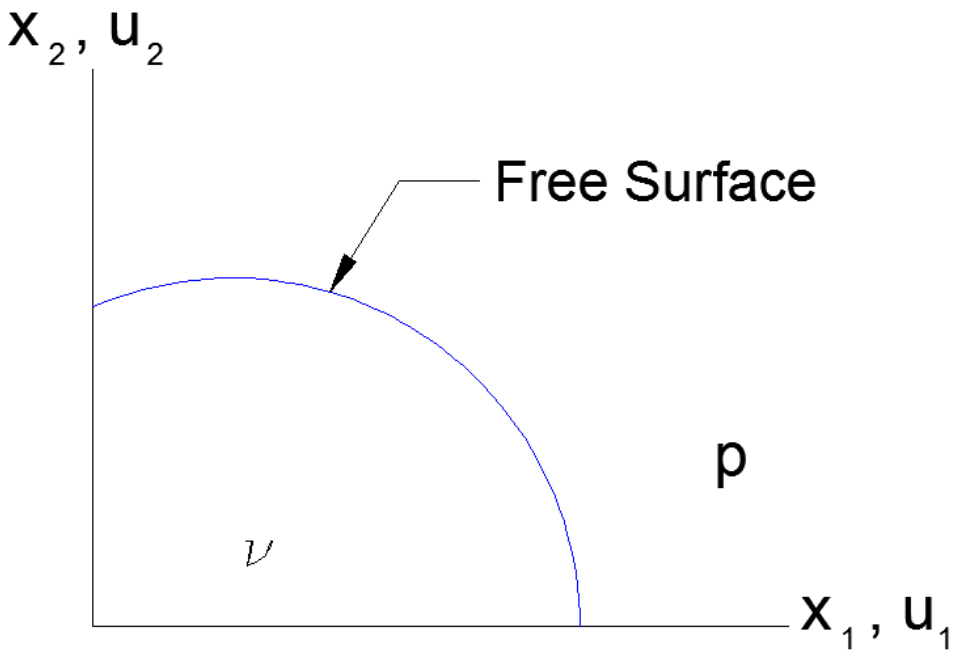


Figure 6: Display of 2-Dimensional Geometry

$$\frac{\partial u_1}{\partial x_1} + \frac{\partial u_2}{\partial x_2} = 0 \tag{7}$$

$$\mu\left(\frac{\partial^2 u_1}{\partial x_1^2} + \frac{\partial^2 u_1}{\partial x_2^2}\right) - \frac{\partial p}{\partial x_1} = 0 \tag{8}$$

$$\mu\left(\frac{\partial^2 u_2}{\partial x_1^2} + \frac{\partial^2 u_2}{\partial x_2^2}\right) - \frac{\partial p}{\partial x_2} = 0 \tag{9}$$

$$p - 2\mu\left(\frac{\partial u_1}{\partial x_1} + \frac{\partial u_2}{\partial x_2}\right) = p_0 - \sigma \mathrm{K} \tag{10}$$

Where K is the free surface curve given by $\frac{1}{R}$ for the 2-D case, and p_0 is the atmospheric pressure outside the fluid body.

There exists a unique solution for equations (7-10) in terms of the fluid velocity field $\boldsymbol{u} = (u_1, u_2)$, given in the integral form (Ladyzhenskaya, 1963):

$$c_{ij}u_j(x_i) + \int_{\Gamma} q_{ij}(x_i, y_i)u_j d\boldsymbol{\Gamma}_{\mathbf{y}} = \int_{\Gamma} s_{ij}(x_i, y_i)b_j d\boldsymbol{\Gamma}_{\mathbf{y}} \tag{11}$$

$$c_{ij}\left\{= \delta_{ij}, x \in \Omega; = \frac{\delta_{ij}}{2}, x \in \Gamma, = 0; x \in \Omega'\right\} \tag{12}$$

$$q_{ij}(x_i, y_i) = \frac{r_i r_j}{\pi R^2} r_k n_k \tag{13}$$

$$s_{ij} = \frac{1}{4\pi}\left[\frac{r_i r_j}{R^2} - \delta_y \log\, R\right] \tag{14}$$

where y_i is the position vector of the free surface and x_i is any point in the interior of the fluid, $(i = 1,2)$ and $(j = 1,2)$ are the coordinate directions, $r_i = x_i - y_i$, $R = \sqrt{r_1^2 + r_2^2} = |x - y|$, and Ω' is the complementary region given by $\Omega \cup \Gamma$. The solution of equation (11) is in non dimensional form with the scales for the velocity, pressure and time given as:

$$V_s = \frac{\sigma}{\mu} \tag{15}$$

$$p_s = \frac{\sigma}{L} \tag{16}$$

$$t_s = \frac{L\mu}{\sigma} \tag{17}$$

where L is an appropriate length scale for the geometry being analyzed. The equation (11) can be rewritten in the fallowing symbolic notation:

$$Cu(x) + \int_{\Gamma} Q(x, y)u d\Gamma_{\eta} = \int_{\Gamma} S(x, y)b d\Gamma_{\eta} \tag{18}$$

where C, Q, and S are the second rank tensors whose elements are c_{ij}, q_{ij}, and s_{ij} respectively. For a unique solution to exist this equation must be solved together with the constraint that the fluid mass must be conserved at the free surface represented by:

$$\int_{\Gamma} u d\Gamma_{\eta} \tag{19}$$

These two equations represent the basic mathematical model for the coalescence of two infinitely long fluid cylinders in a two dimensional Cartesian coordinate system.

Axis-Symmetric Geometry

The two dimensional case is not accurate in describing the behavior of spherical droplets, so the process is modified in order to describe the actual behavior. This is accomplished by transforming the two dimensional case into the cylindrical coordinate system using the following transformation:

$$x_i = (x_1, x_2, x_3)^T = (r\cos\theta\,, r\sin\theta\,, z)^T \tag{20}$$

Then the tensor functions, c_{ij}, q_{ij}, ands_{ij}, must be written for $\mathrm{i,j} = 1,2,3$ in the following way:

$$c_{ij} = \begin{Bmatrix} \delta_{ij} & x \in \Omega \\ \dfrac{\delta_{ij}}{2} & x \in \Gamma \\ 0 & x \in \Omega' \end{Bmatrix} \tag{21}$$

$$q_{ij}(x_i, y_i) = \frac{3(x_i - y_i)(x_j - y_j)(x_K - y_K)n_K}{4\pi|x - y|^5} \tag{22}$$

$$s_{ij} = \frac{1}{8\pi}\left[\frac{\delta_{ij}}{|x-y|} + \frac{(x_i - y_i)(x_j - y_j)}{|x-y|^3}\right] \tag{23}$$

where x represents an interior point and y represents the free surface location. Axial symmetry can be assumed so that $u_\theta = 0$ and only u_r and u_z need to be evaluated at the intersection of the surface $\delta\Omega$ with the half space $\theta = 0$. After substitution of the cylindrical coordinates into equation (11) for the Cartesian case the integral equation for the cylindrical case becomes:

$$c_{\alpha\beta}u_\beta^c + \int_\Gamma q_{\alpha\beta}^c u_\beta^c d\Gamma = \int_\Gamma s_{\alpha\beta}^c b_\beta^c d\Gamma \tag{24}$$

where superscript c stands for cylindrical coordinates and α and β are either 1 or 2, therefore $u^c = (u_1^c, u_2^c)^T = (u_r, u_z)^T$, the coefficients $q_{\alpha\beta}^c$ and $s_{\alpha\beta}^c$ can be written in terms of complete elliptical integrals of the first and second kind (Vorst & Mattheij, 1995). A computer program was then developed by Antar, Ethridge and Maxwell to determine a numerical solution to the above equation. This program is described in the next chapter.

NUMERICAL SOLUTION

In the previous chapter the governing equations for the coalescence process were derived in the form of the integral equations:

$$c_{\alpha\beta}u_{\beta}^{c} + \int_{\Gamma} q_{\alpha\beta}^{c}u_{\beta}^{c}d\Gamma = \int_{\Gamma} s_{\alpha\beta}^{c}b_{\beta}^{c}d\Gamma \tag{25}$$

$$\int_{\Gamma} u^{c}\, d\Gamma \tag{26}$$

where:

$$c_{ij} = \begin{cases} \delta_{ij} & x \in \Omega \\ \dfrac{\delta_{ij}}{2} & x \in \Gamma \\ 0 & x \in \Omega' \end{cases} \tag{27}$$

$$q_{ij}(x_i, y_i) = \frac{3(x_i - y_i)\left(x_j - y_j\right)(x_K - y_K)n_K}{4\pi|x - y|^5} \tag{28}$$

$$s_{ij} = \frac{1}{8\pi}\left[\frac{\delta_{ij}}{|x - y|} + \frac{(x_i - y_i)\left(x_j - y_j\right)}{|x - y|^3}\right] \tag{29}$$

Equations (25-29) are in the form of an integral equation bounded by the free surface. These equations can be solved using Finite Element Methods (FEM), and since these equations are integrals over the boundary, Boundary Elements Methods (BEM) (an offshoot of FEM) can be used to determine a numerical solution to the problem. In order for the results of the numerical solution to be used for all materials, the material properties were substituted by non-dimensional variables. The equations for non-dimensionalization of the time are as follows:

$$t^* = \frac{t}{t_s} \Rightarrow t = t_s t^* \tag{30}$$

$$t_s = \frac{L\mu}{\sigma} \tag{31}$$

where t^* is the non-dimensional time, t is the physical time, t_s is the time scale, and L is the characteristic length scale, in this case the initial radius of the droplets. The equations for the non-dimentionalization of the length scale are as follows:

$$l^* = \frac{l}{l_s} \Rightarrow l = l_s l^* \tag{32}$$

where l^* is the non-dimensional length, l is the physical length, and l_s is the length scale, taken as the initial diameter of the droplets in these calculations.

Methodology

For solving the equations using BEM the boundary must be subdivided into separate evenly spaced points. The equations are then solved for the velocity field for each of these points. This velocity field can then be integrated with respect to time, at each time step, in order to determine the new location for the boundary points using the following equation:

$$x = \int u(x)dt \tag{33}$$

This will show the evolution of the free surface as the droplets coalesce. A characteristic measurement must be selected so that the evolution of the process can be measured. An appropriate measure is the variation of the contact radius over time.

Computer Programs

In order to perform this analysis, three computer programs were developed (Antar, Ethridge, & Maxwell, 2003); an initial surface geometry generator, a double symmetry simulator, and a single symmetry simulator. Because of computational difficulties when the initial contact radius is set to a very small value, it is necessary to set it to $0.1 \times D_0$, where D_0 is the initial diameter of the drops in order to achieve a solution. If the time steps used in the initial calculations are handled correctly this should not have an effect on the outcome of the data (Antar, Ethridge, & Maxwell, 2003).

Surface Geometry Generator

The initial surface geometry generator was created to produce evenly spaced surface points. The number of points desired is inputted by the user. The evenly spaced element points are then determined by spacing the points at even angles about the center point of the droplets. The points are then outputted into a text file. The points are viewed using Microsoft Excel in order to verify that the geometry generated properly. The text file can then be used in one of the other two programs for calculations.

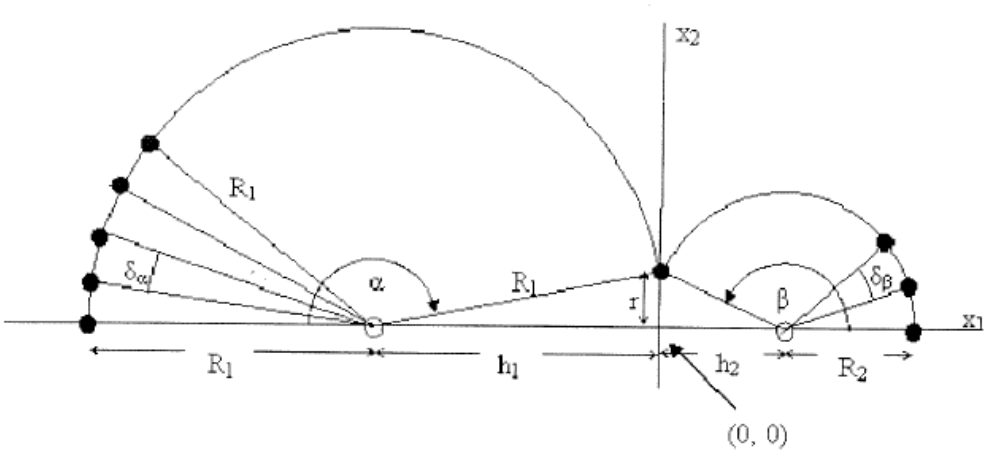


Figure 7: Surface Point Generator Point Location, for Single Symmetry Case

Double Symmetry Simulator

For calculations for equal sized drops double-symmetry can be used. This means that along with axial symmetry the process is symmetric about the line of radial contact. Therefore, only one fourth of the surface geometry needs to be calculated saving processor time (Figure 8). This is the program used to determine the appropriate theoretical curve of the contact radius for the experiments that are analyzed in this thesis. The results of this program are presented in Figure 9. Figure 10 shows the progression of the droplets as they coalesce.

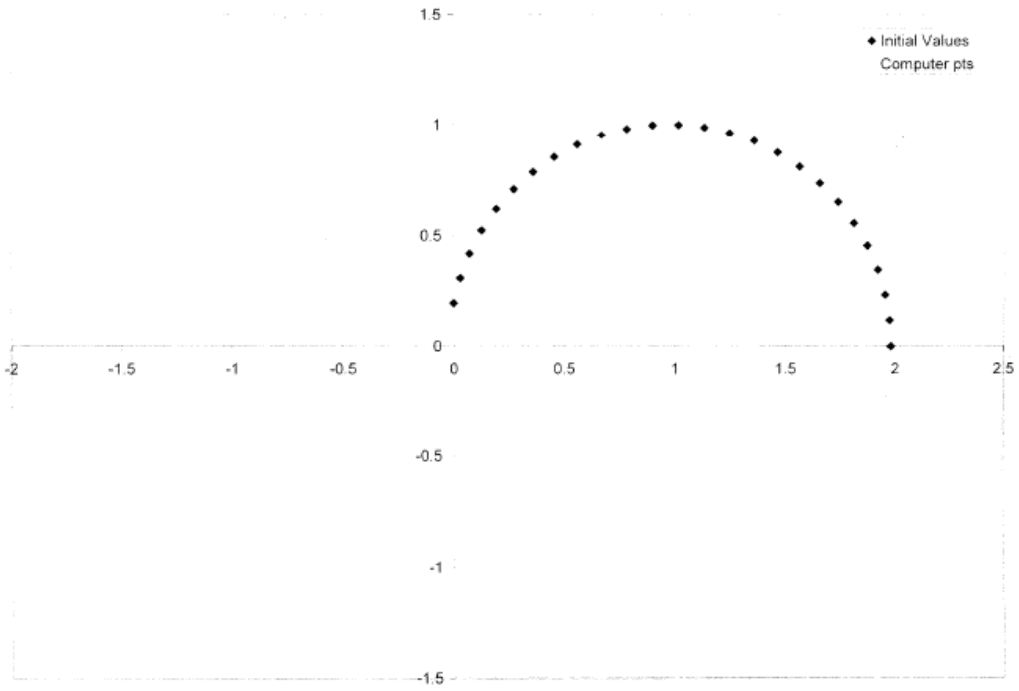


Figure 8: Points for Double Symmetry Case (Lehman, 2005)

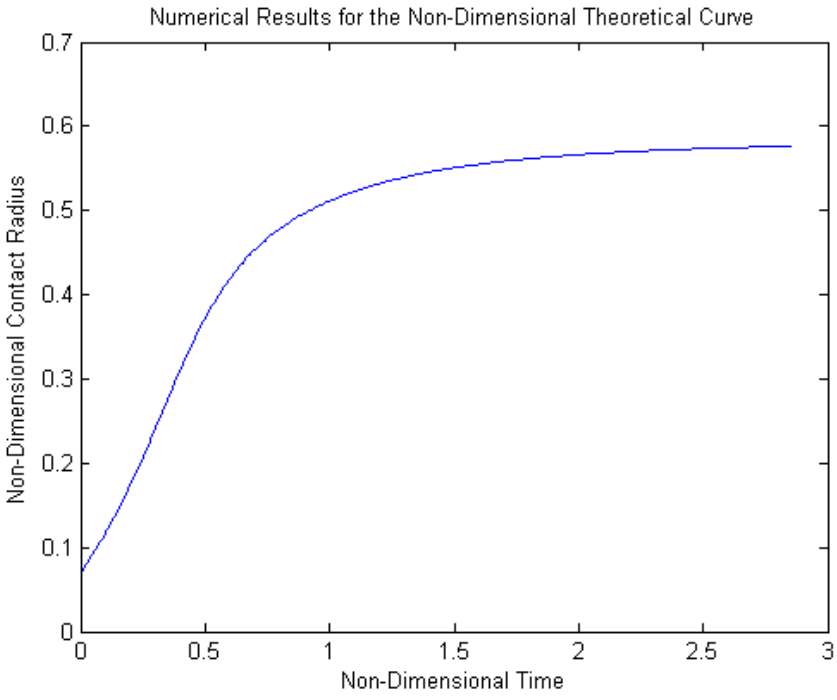


Figure 9: Theoretical Curve for Double Symmetry

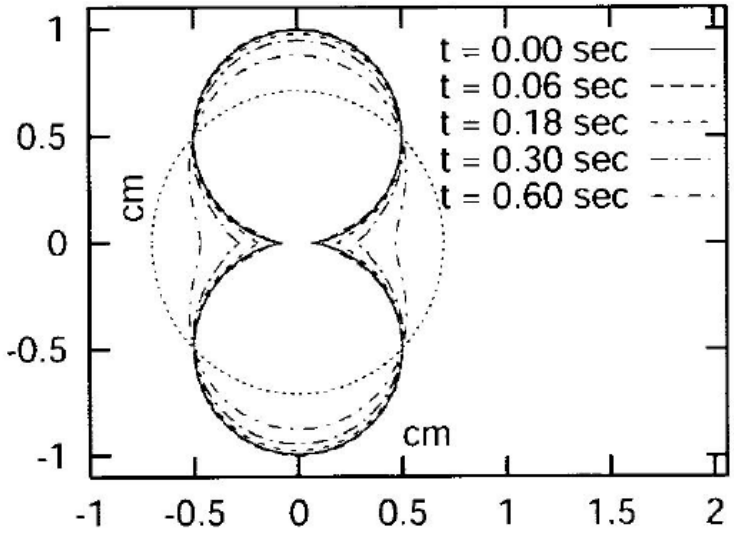


Figure 10: Progression of Two Equal Drops over Time (Antar, Ethridge, & Maxwell, 2003)

Single Symmetry Simulator

The single-symmetry simulator was used for calculating the coalescence of two different sized droplets (Figure 7) because the calculations can only be made symmetric about the axis. This program calculated the coalescence using only the axial symmetry. Experiments were run using different sized droplets; however, the videos were not available for analysis. Figure 11 shows the progression of the droplet merger as they coalesce.

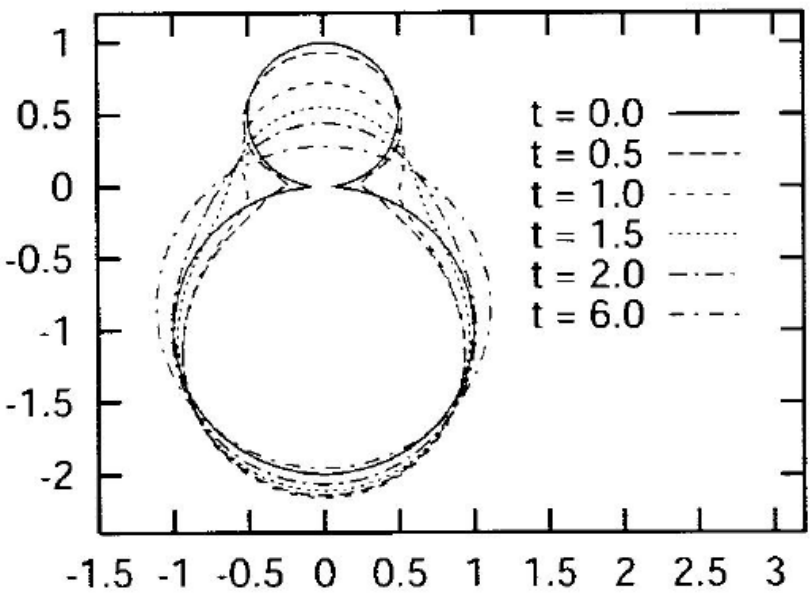


Figure 11: Progression of Two Unequal Drops over Time (Antar, Ethridge, & Maxwell, 2003)

EXPERIMENTAL SET UP

KC-135 Tests

Experiments performed on the KC-135 experienced a lot of g-jitter. The experiment had to be designed so that it can be set up and run in the 20 seconds of microgravity the KC-135 provides each cycle. In these experiments two drops were supported by two hypodermic needles (Figure 12). After the drops were formed on the end of the needles they were brought together and allowed to coalesce (Figure 13). The presence of the needles introduced a different geometry to the droplets. This, along with the g-jitter, complicates the calculations and introduces errors into the results.

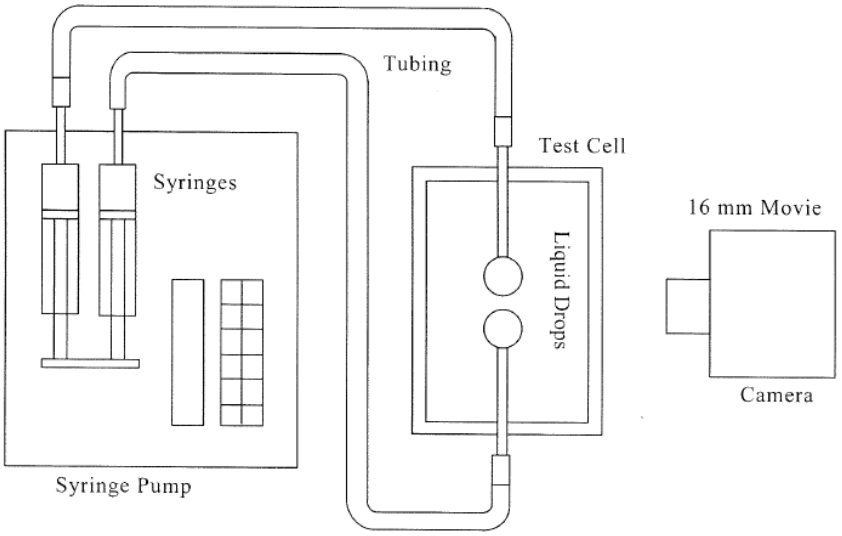


Figure 12: KC135 Experimental Setup (Lehman, 2005)

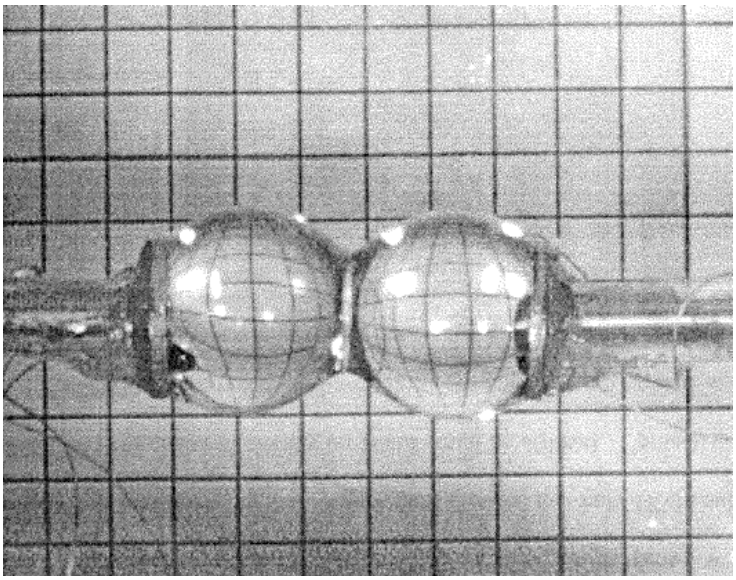


Figure 13: Photo of Experiment Being Carried Out on the KC135

ISS Tests

The experiments that were analyzed for this paper were performed on the ISS in August 2003 by American Astronaut Mike Ficke. The experiment was performed on the ISS because the station provided a stable long term microgravity environment. These experiments were constrained by having a limited mass that was designated to send to the station of only 1 kg. Therefore, the experiment was designed to utilize as much equipment as possible that is already aboard the station. The equipment that was sent to the station included a background sheet with a 1 cm square grid and syringes filled with predetermined amounts of various liquids. The equipment that was used that was available to the astronauts and already on the station was a frame to hold the background grid, the digital video camera running at 29.97 frames per second, a hand held flashlight, some string from a sewing kit, and some tape (Figure 14).

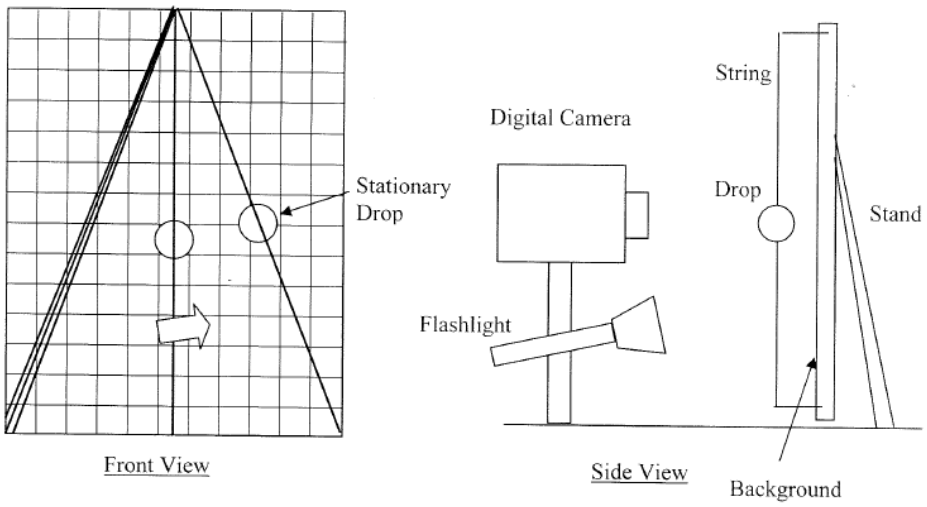


Figure 14: ISS Experimental Setup

For the experimental setup, the grid background was attached to the frame and strings were attached using tape to the outside of the frame. The camera was mounted so that it pointed at where the drops would be. The flashlight was mounted so that it shows directly onto the background. The string is taped at the ends to the front of the frame.

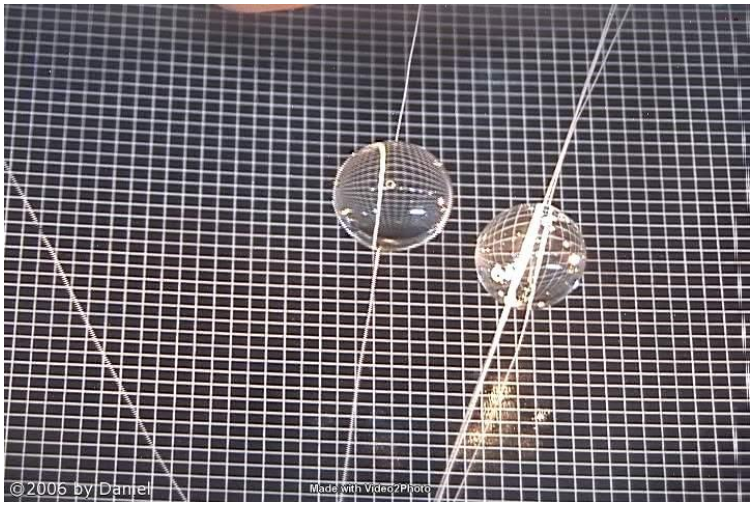


Figure 15: Experiment Being Carried Out on ISS

The experiments that were analyzed for this report used silicon oil at approximately 12,500 CP. To perform the experiment 2 strings were separated and attached to the frame with tape. A 1.0 cc drop of oil was deposited on each string (Figure 15). Leaving one string taped in place, the two drops were brought together by moving the other string. When the drops began to coalesce the tension was released from the second string so that the drops would come together on their own. When the drops are fully coalesced the two strings are put together and taped in place.

A third string is separated and a 2 cc drop is deposited onto the third string. This string is then used to move the 2 cc drop into the 2 cc drop from the first run. Again when the drops begin to coalesce, the tension is removed from the third string and the drops are allowed to come together. Then the three strings are taped together and a fourth string is separated. A 4 cc drop is deposited on the string and brought together with the drop from the previous run. Finally a fifth string is separated and a 8cc drop is deposited on it and brought together with the drop from the previous runs.

Experiments were also run with 100,000 cp silicon oil, glycerin, and honey, a non Newtonian fluid. Tests were attempted with corn syrup, however a thin skin developed on the outside of the drops when they were exposed to air which prevented the drops from coalescing. The videos for these other experiments were not provided in order to analyze them.

Table 1: List of Fluid Properties for Experiments on the KC135 and ISS (Lehman, 2005)

Fluid	Density g/cc	Surface Tension N/m	Viscosity N s/m^2
glycerin	1.17	0.063	629-1490
Silicone Oil	0.97	0.0215	12500
Silicone Oil	0.97	0.0215	100000
Honey	1.45	90	12500-100000
Corn Syrup	1.41	0.083	2200-15000

ANALYSIS

Automated Analysis Difficulties

The analysis performed on the videos to determine the contact radius, was done using Matlab. An automated program for performing the analysis was attempted however it was not possible due to three reasons. The first reason is that the black background for the movies with white lines made isolating the droplets from the background nearly impossible for the algorithms provided in the Matlab image processing tool box (Figure 16). The second issue was the lighting. The glare from the lights made it difficult to detect the contact edge of the droplets in both the automated methods and the manual selecting methods that were employed (Figure 17).

The glare also contributed to the difficulty in isolating the droplets from the background. The third reason an automated program couldn't be written is because the strings that stabilized and directed the droplets contrasted too much with the background contributing to the difficulty in isolating the drops.

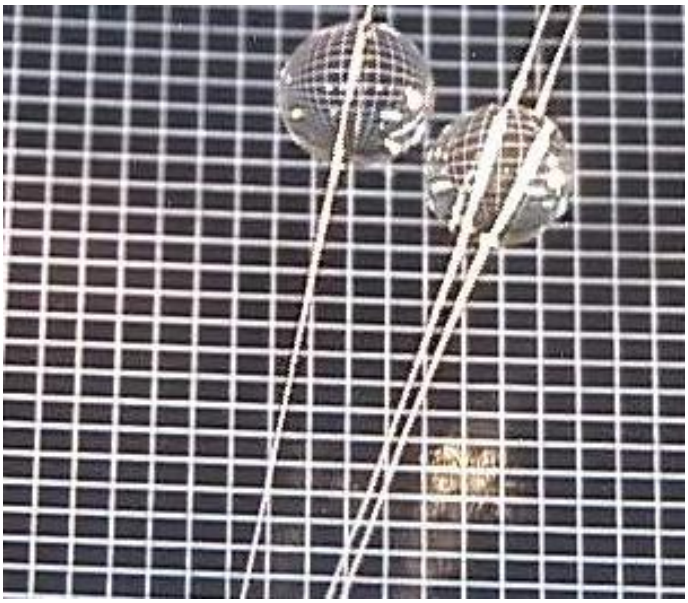


Figure 16: Inconsistencies in Background Color and Intensity



Figure 17: Glare and Support Strings Causing Difficulties in Locating Contact Points

Acquiring Data

Preparing Videos

In order to prepare the videos, they needed to be imported into Matlab. Due to the large amount of data in the videos they needed to be shortened in length so that they only included the time from a few frames before the droplets made contact to where the droplets were sufficiently combined to provide enough data for analysis. Also in order to save computer memory and make it easier to determine the contact radius, the videos were cropped to a size that only the area where the droplets are shown during the length of the video.

Measuring Contact Diameter

After the videos were prepared a graphical user interface (GUI) was created in Matlab so that the contact diameter can be determined from the images (Figure 18). First a measurement of the grid spacing was taken so that a length scale can be determined for each video (Figure 19). Using the 'impoint' command in Matlab the point of contact on either side of the contact radius was located (Figure 20). Due to glare from the lighting this was difficult on almost all of the videos. An approximate location had to be selected, and all the frames were used in order to attempt to eliminate any error that might occur due to resolution and glare. After the two contact points were located in each frame the distance between those two points is calculated giving the contact diameter which is then analyzed to determine the viscosity of the fluid (Figure 21).

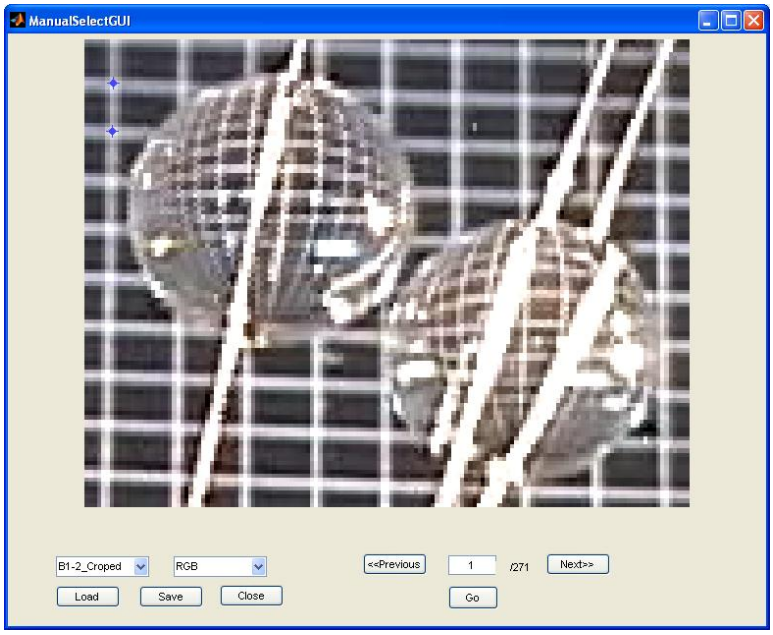


Figure 18: Graphical Interface for Selecting Points for Contact Radius

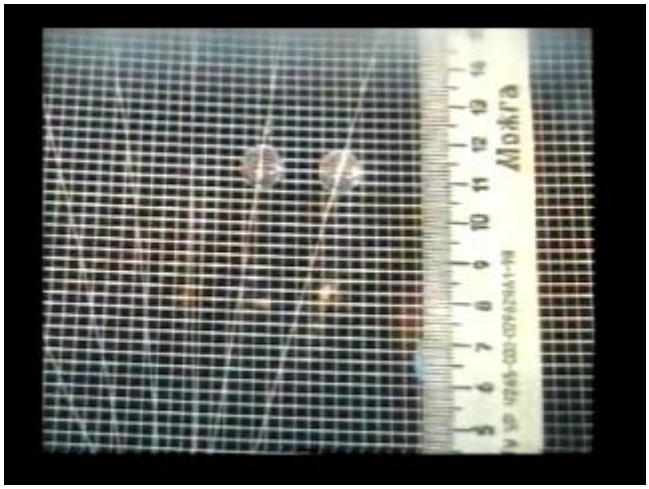


Figure 19: Scale Photo for Determining Length Scale for Photos

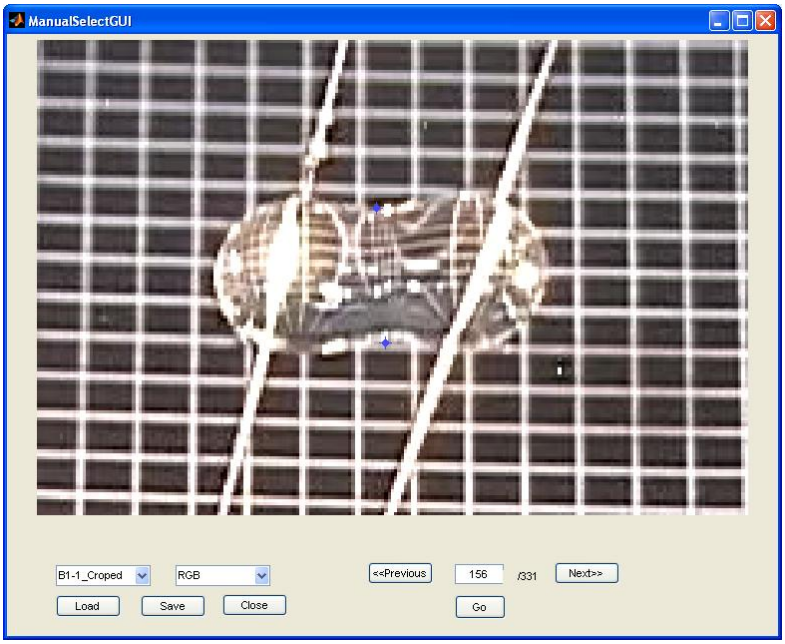


Figure 20: Location of Contact Points for Calculating Contact Radius

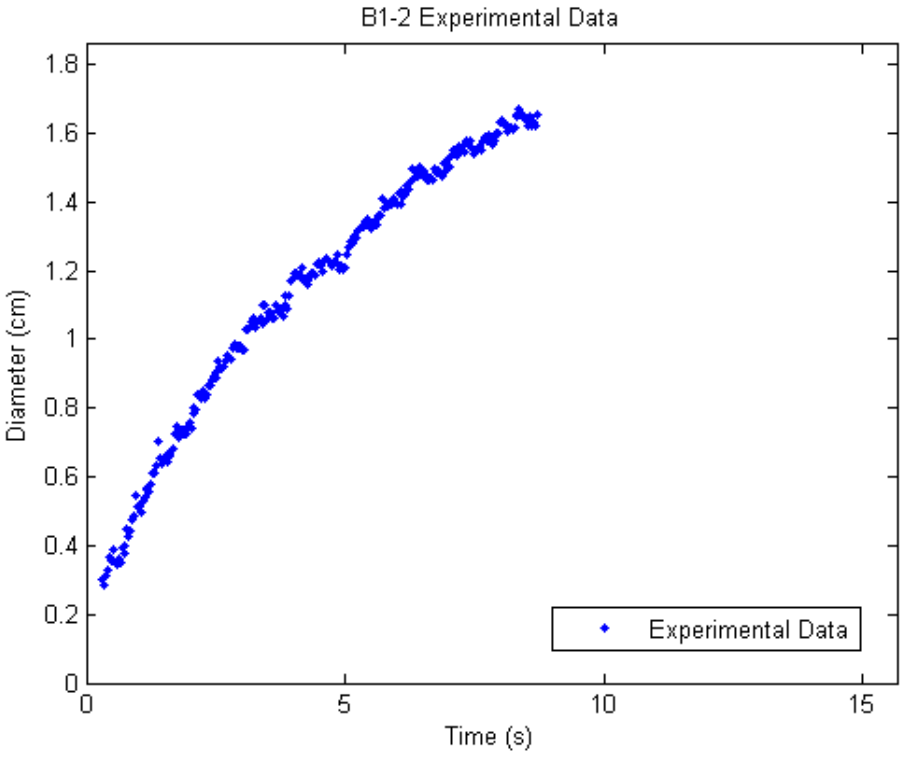


Figure 21: Resulting Experimental Data

Analyzing the Data

Another GUI was created to help determine the Viscosity of the Fluid from the data from the previous program (Figure 22). After scaling the data for the contact diameters by the scale for each movie the theoretical data can then be converted into its dimensional form corresponding to the initial droplet size for each experiment using the following equation.

$$D_{th} = 2\, R_{th}^{*}\, D_0 \tag{34}$$

$$t_{th} = (t_{th}^{*} - t_0)\, D_0\, \frac{\mu}{\sigma} \tag{35}$$

where R_{th}^{*} is the non-dimensional contact radius, D_{th} is the dimensional contact diameter, t_{th}^{*} is the non-dimensional time, t_{th} is the dimensional time, σ is the known surface tension, D_0 is the initial diameter of the droplets, and the variables μ and t_0 are estimations of the viscosity and initial time constant respectively. The theoretical curve is adjusted by changing the viscosity value μ, to match the curve of the experimental data, so that the curves match in steepness (Figure 24). Since the initial time of contact is difficult to determine and the theoretical data does not start until the contact radius is $0.1 \times D_0$ an arbitrary initial time, t_0, is chosen. This time constant is then adjusted (Figure 23) so the initial value of the experimental data that is being analyzed, falls on the curve for the theoretical data. This time constant has no effect on the value of the viscosity measurements. The values of the viscosity and initial time constant are adjusted repeatedly, until the data closely matches the theoretical curve. This provides a good estimate of the value for the viscosity; however, if a more refined value is needed, a command has been written to utilize the ‘fminbnd’ command in

Matlab in order to determine the best fit for the data to the theoretical curve. The 'fminbnd' command utilizes the Simplex method to determine the minimum point for a function with two or more variables.

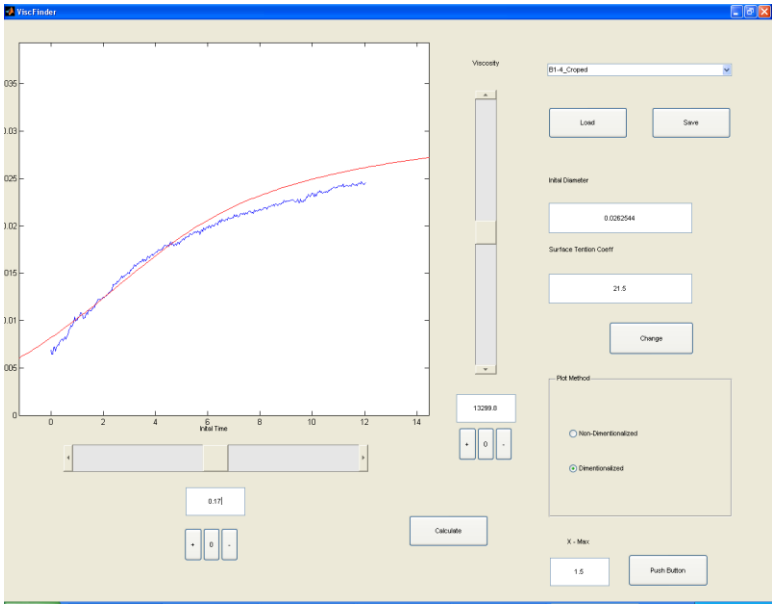


Figure 22: Graphical Interface for Determining Viscosity

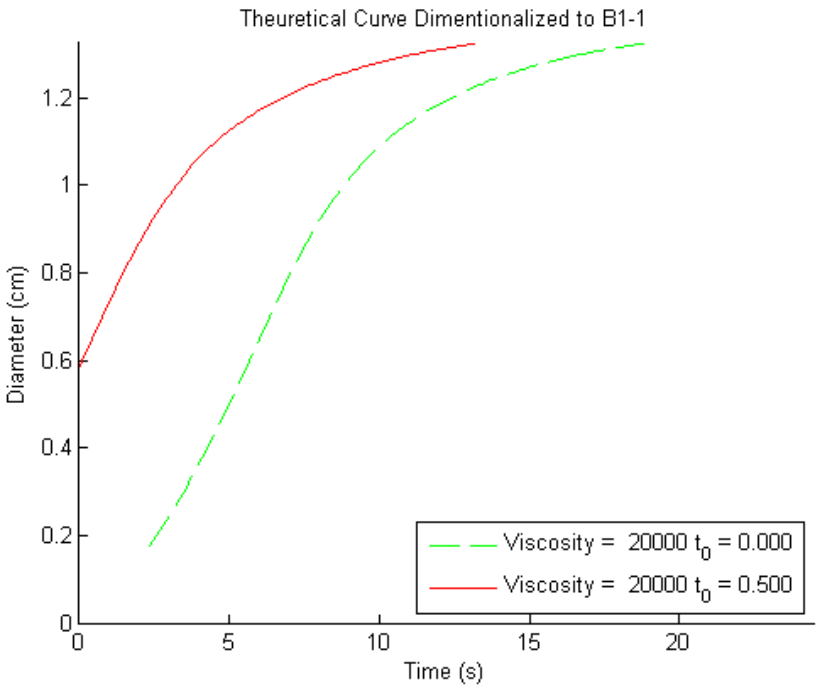


Figure 23: Effects of Changing the Time Constant t_0 on the Theoretical Data

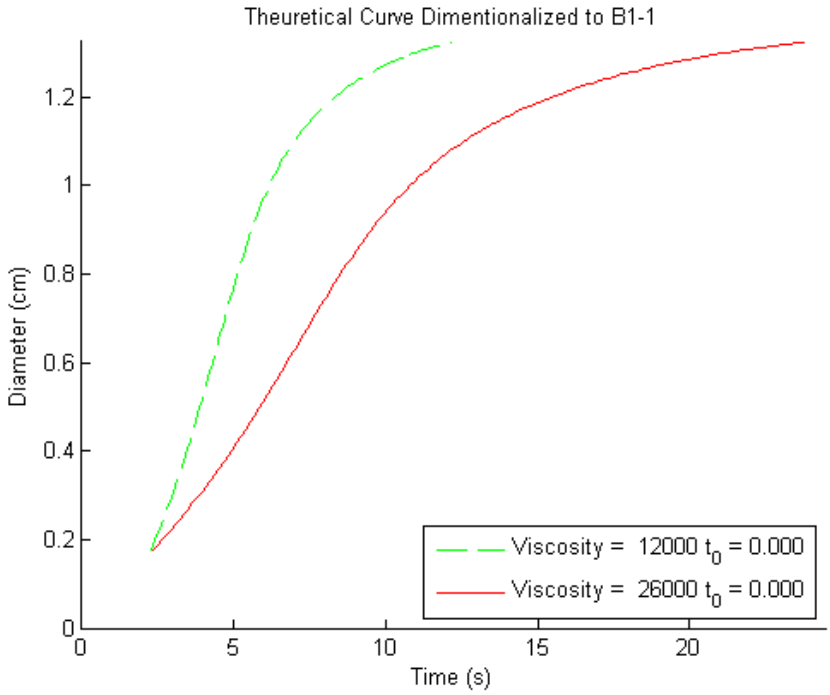


Figure 24: Effects of Changing the Viscosity on the Theoretical Data

RESULTS AND CONCLUSIONS

When attempting to fit the theoretical curve to the data, there were some discrepancies between the initial part of the data curve and the final part of the theoretical data. Therefore, the curve was fit to both the initial portion of the data and the final portion, along with the fit for the overall curve. The results of these fits are stated in Table 2 and will be discussed in detail. The manufacturer provided value of 12500 Ns/m^2 for silicone oil, is presumed for these measurements. However, there may be some discrepancy due to temperature effects that could not be accounted for with known data. Also a value of the surface tension σ, is specified by the manufacturer as 0.0215 $\frac{N}{m}$.

Table 2: Viscosity Results For all Samples

		Viscosity		
Sample	D0	Overall	Initial	Final
	cm	N s/m^2		
B1-1	1.2045	26090	15670	31638
B1-2	1.6892	14679	11292	16030
B1-3	2.1068	x	x	17780
B1-4	2.6254	15963	11046	19674

Individual details

Sample B1-1

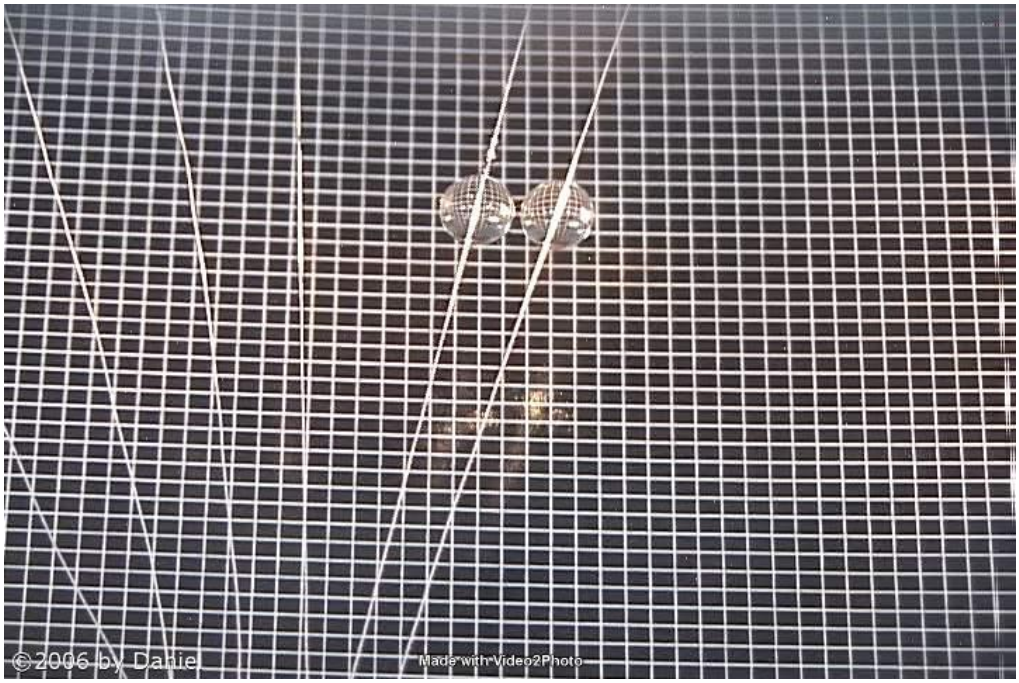


Figure 25: Sample B1-1

Figure 25 shows a frame from the video for the first experiment. In this run two 1cc droplets are coalesced. The overall curve fit for the data curve was at a viscosity of 26300 Ns/m^2 (Figure 26) with the initial data fitting to 15670 Ns/m^2 (Figure 27), and the final data fitting to 31638 Ns/m^2 (Figure 28). Figure 29 shows all three viscosity values with the experimental data.

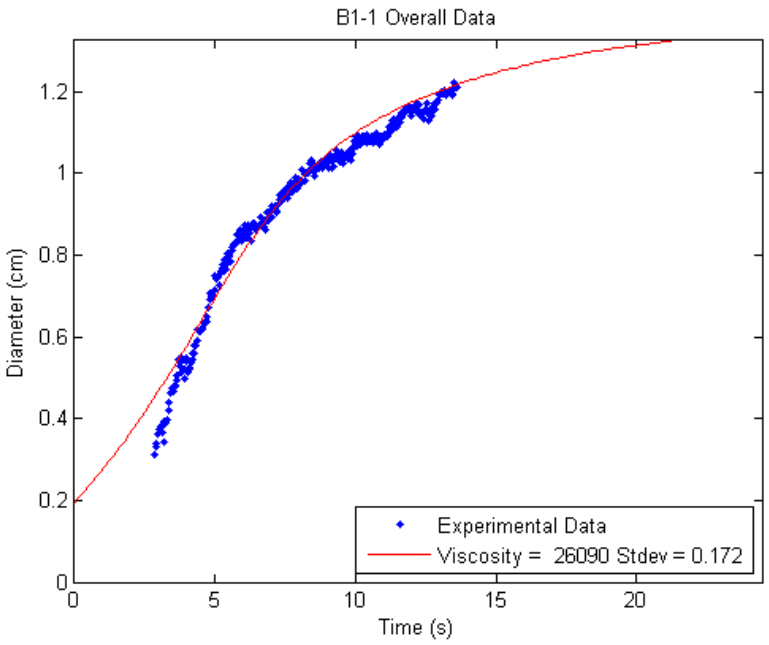


Figure 26: Sample B1-1 Overall Data Fit

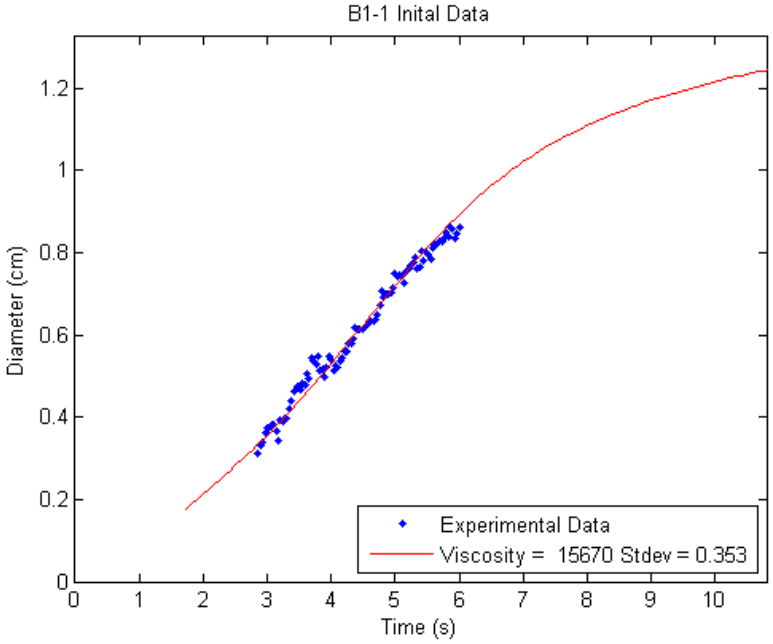


Figure 27: Sample B1-1 Initial Data Fit

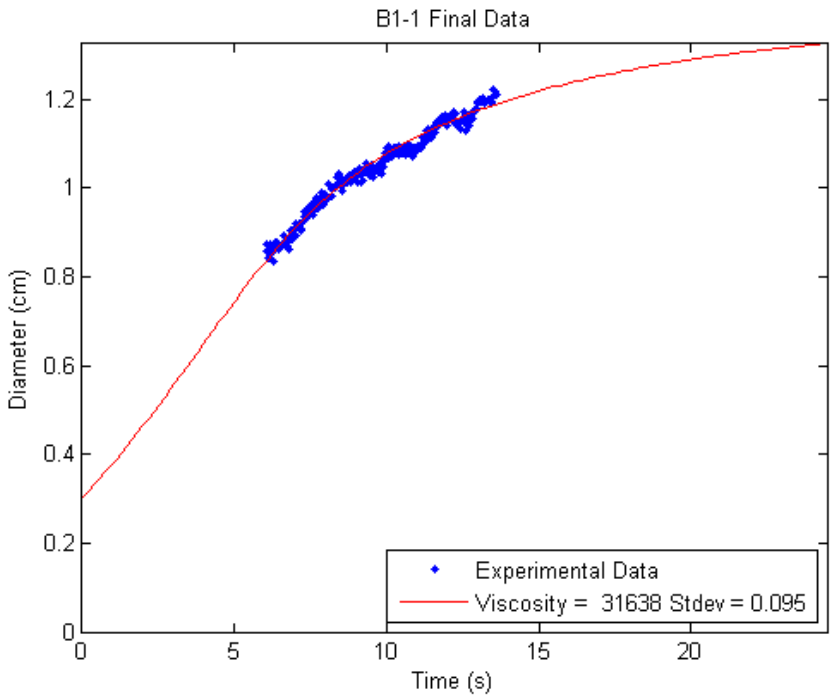


Figure 28: Sample B1-1 Final Data Fit

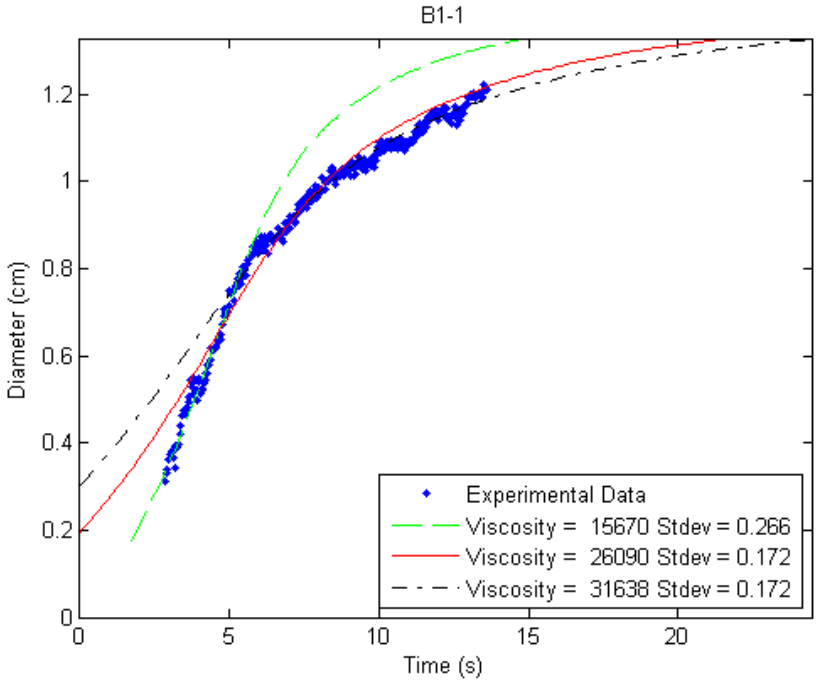


Figure 29: Combined Graph of Measurements for Sample B1-1

The range measured does not correlate to the known value of 12500 Ns/m^2 (Figure 30). One reason for this could be that the string that is used to stabilize the droplet effects the shape of the droplet and interferes with the coalescence process (Figure 31). Therefore it affects the range of the viscosity measurements. This effect is greatly increased due to the small size of the droplets. Another issue caused by the small size of the droplets is that the resolution of the video made it difficult to determine the points of contact on the drops introducing errors. Also the length of time that the smaller droplets take to coalesce makes fewer data points from which to take measurements.

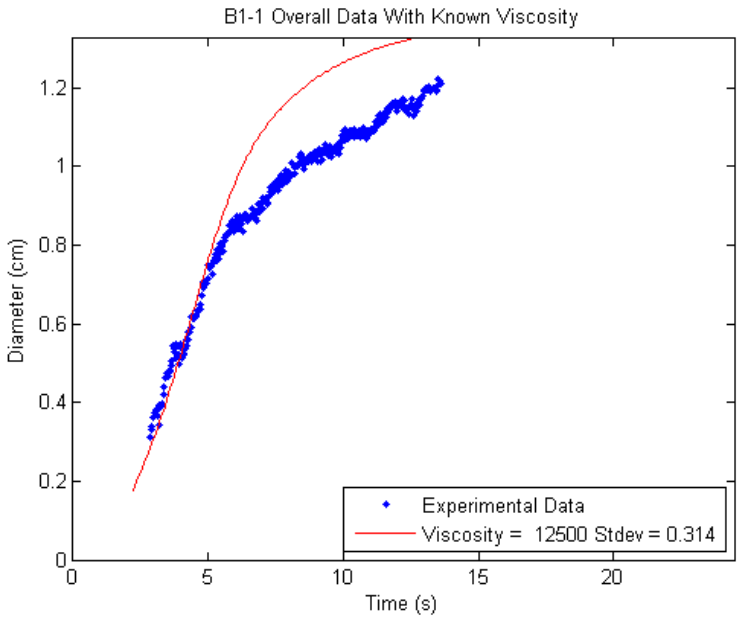


Figure 30: Sample B1-1 with Theoretical Curve for Known Viscosity



Figure 31: Image of Strings Holding Droplets Apart and Effecting Viscosity Measurements

Sample B1-2

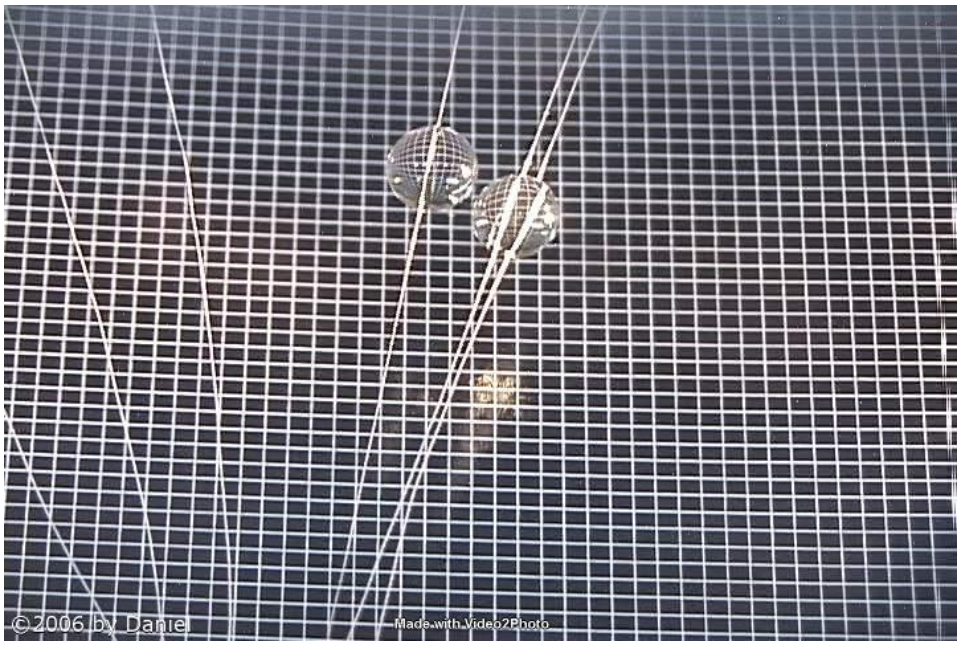


Figure 32: Sample B1-2

Figure 32 shows a frame from the video for the second experiment. In this run two 2cc droplets are coalesced. The overall curve fit for the data curve was at a

viscosity of 14679 Ns/m^2 (Figure 33) with the initial data fitting to 11292 Ns/m^2 (Figure 34), and the final data fitting to 16030 Ns/m^2(Figure 35). Figure 36 shows all three viscosity values with the experimental data.

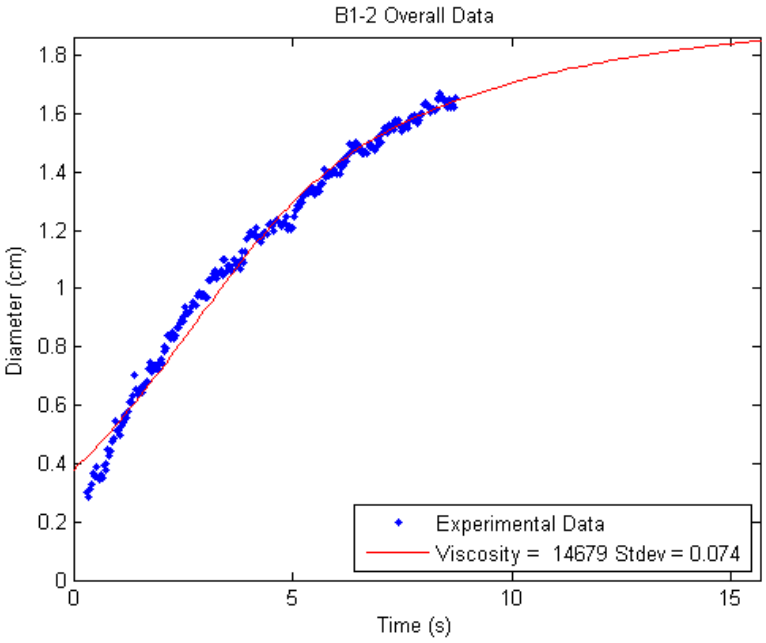


Figure 33: Sample B1-2 Overall Data Fit

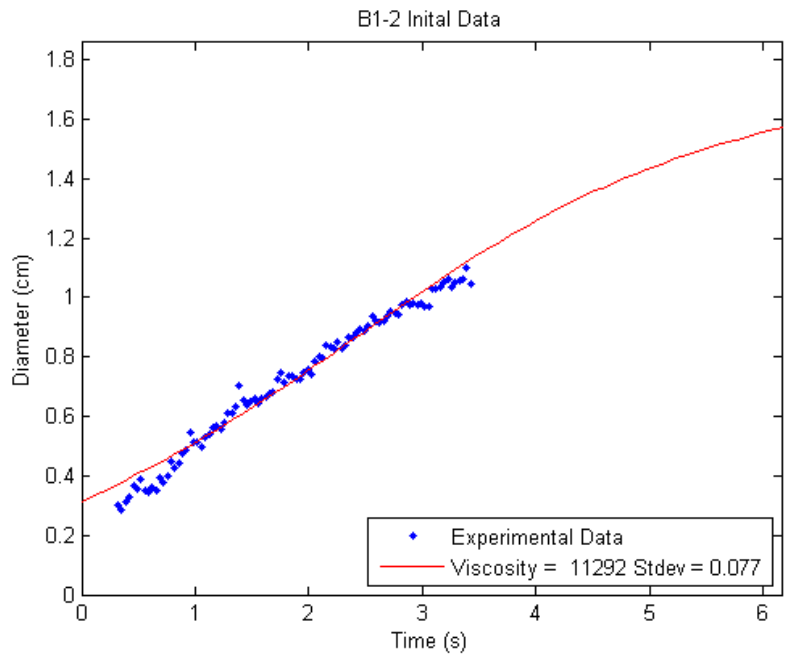


Figure 34: Sample B1-2 Initial Data Fit

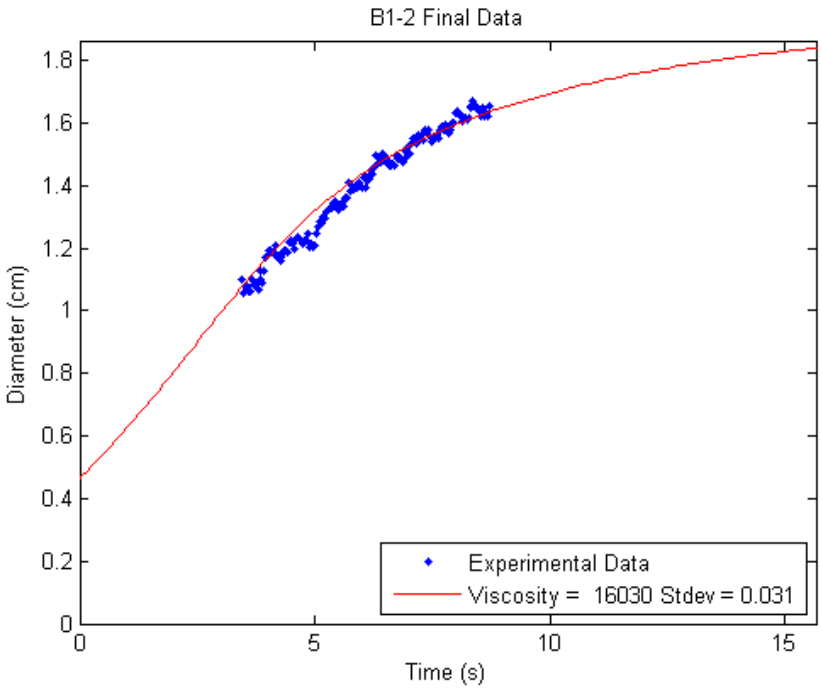


Figure 35: Sample B1-2 Final Data Fit

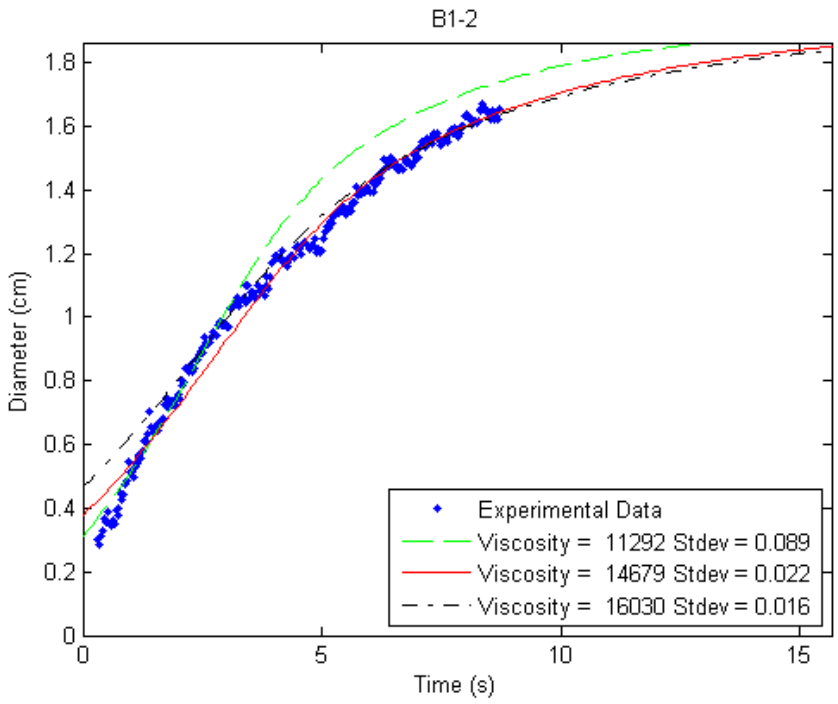


Figure 36: Combined Graph of Measurements for Sample B1-2

The known value of 12500 Ns/m^2 falls within the range of these measurements (Figure 37). As with all of the videos the glare from the lighting has made it difficult to determine the contact point between the two drops. With this video the contact points could be inferred sufficiently from the image to determine fairly accurate data.

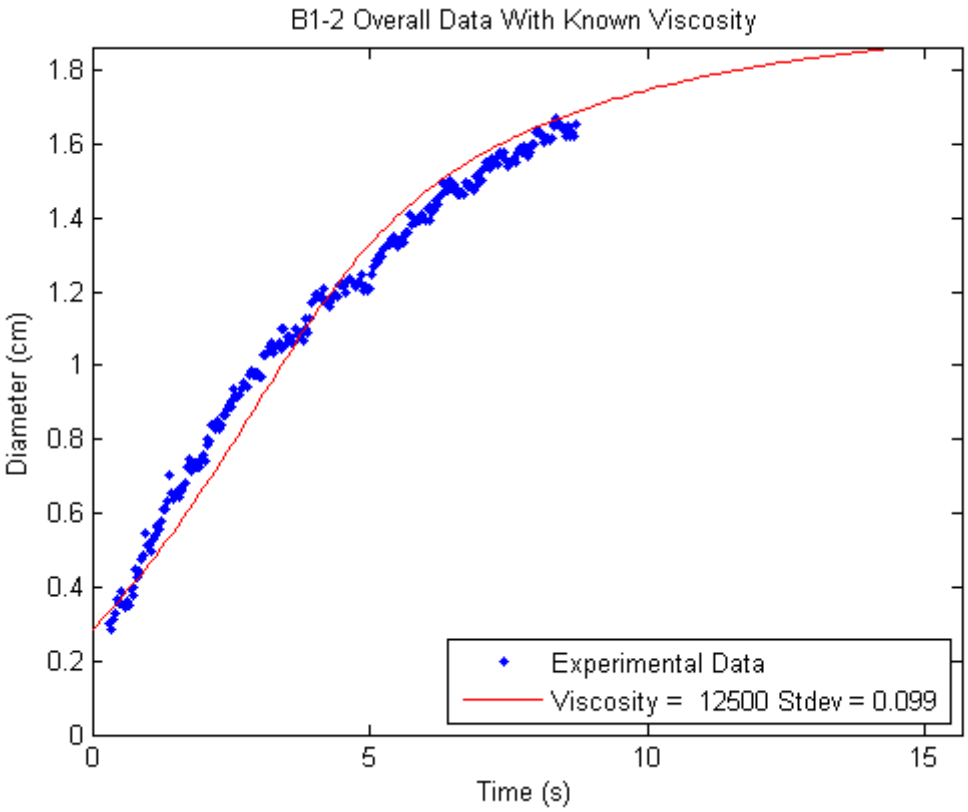


Figure 37: Sample B1-2 with Theoretical Curve for Known Viscosity

Sample B1-3



Figure 38: Sample B1-3

Figure 38 shows a frame from the video for the third experiment. In this run two 4cc droplets are coalesced. The droplets during the initial coalescence were moving around and twisting on the strings (Figure 39), so that only the final data could be fit. The fit for this data corresponded to a viscosity of 17780 Ns/m^2 (Figure 40).

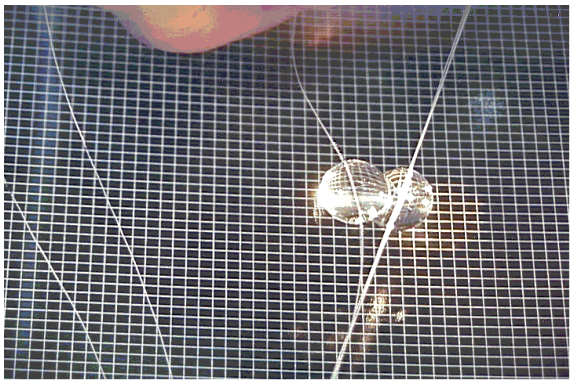


Figure 39: sample B1-3 showing overlap of Droplets during Initial Coalescence

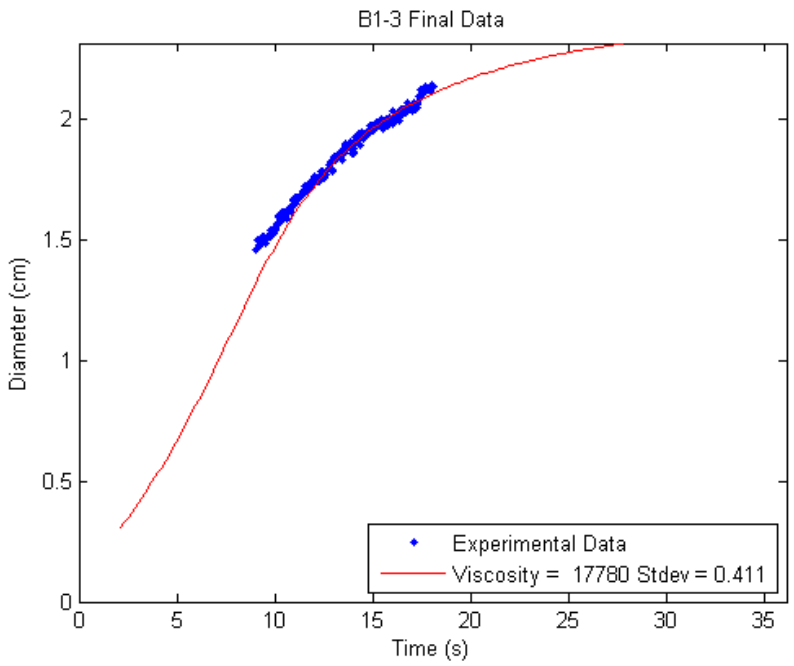


Figure 40: Sample B1-3 Final Data Fit

Sample B1-4

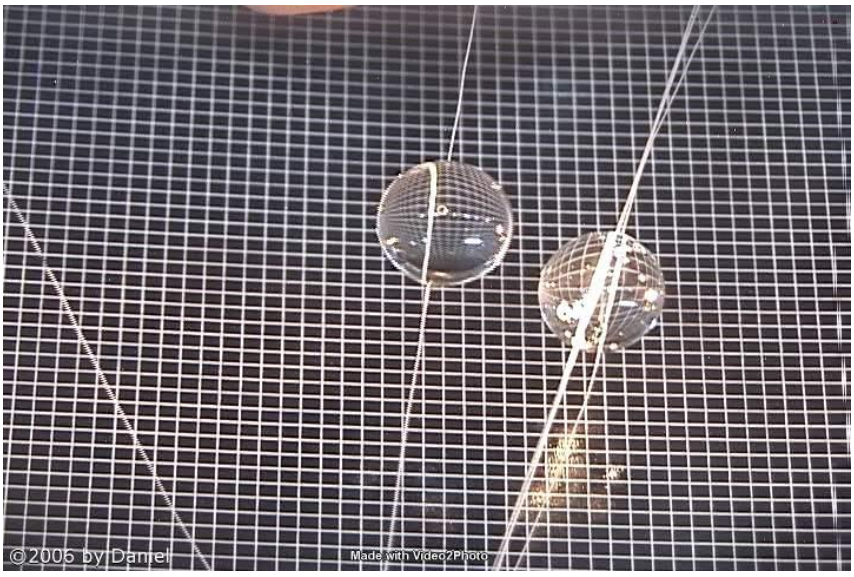


Figure 41: Sample B1-4

Figure 41 shows a frame from the video for the fourth experiment. In this run two 8cc droplets are coalesced. The overall curve fit for the data curve was at a viscosity of 15963 Ns/m^2 (Figure 42) with the initial data fitting to 11046 Ns/m^2 (Figure 43), and the final data fitting to 19674 Ns/m^2 (Figure 44). Figure 45 shows all three viscosity values with the experimental data.

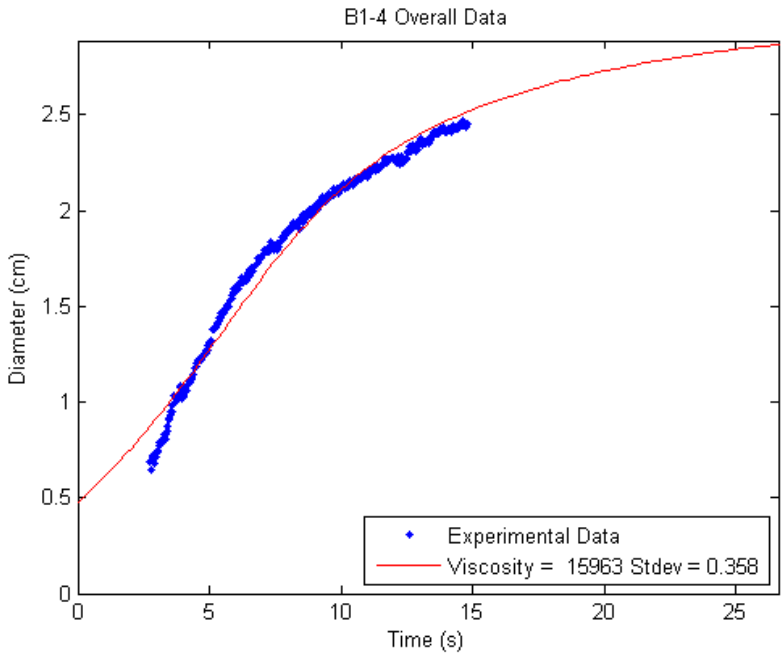


Figure 42: Sample B1-4 Overall Data Fit

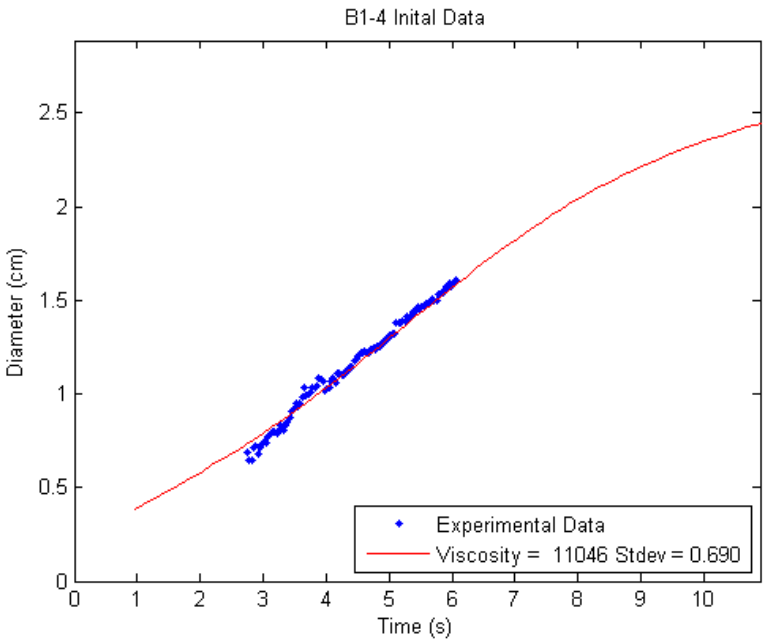


Figure 43: Sample B1-4 Initial Data Fit

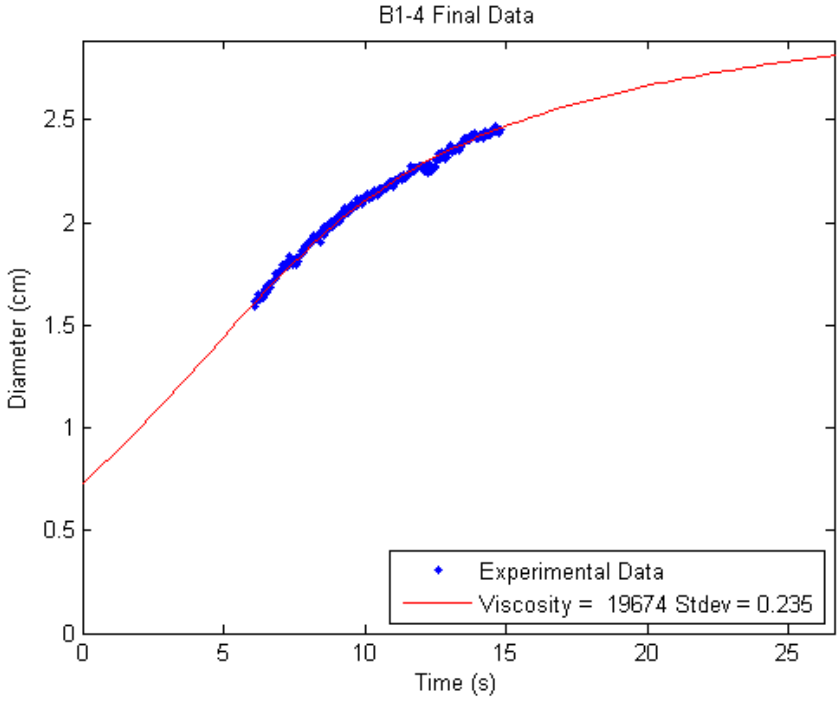


Figure 44: Sample B1-4 Final Data Fit

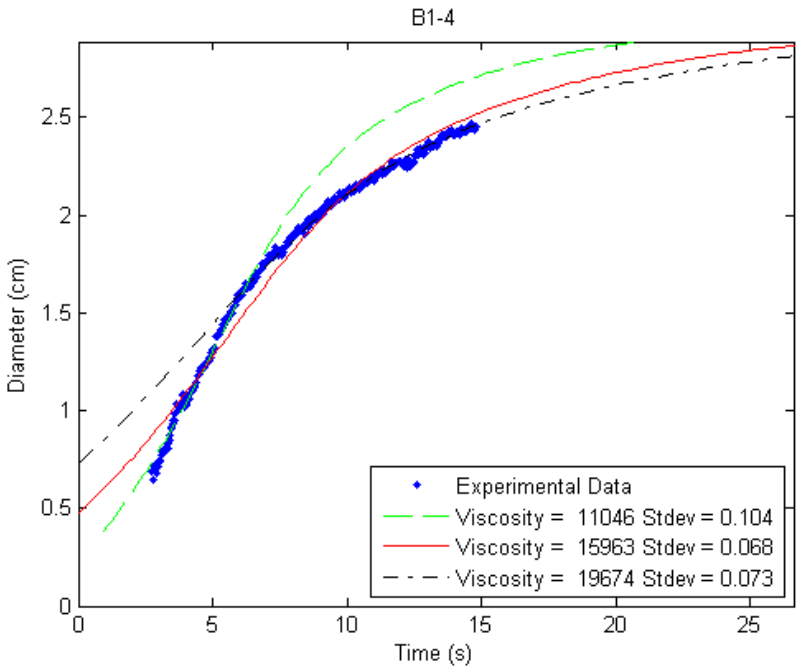


Figure 45: Combined Graph of Measurements for Sample B1-4

The known value of 12500 Ns/m^2, falls within the range of these measurements (Figure 46). However, the range is slightly greater than the range of the B1-2 sample with the initial data nearly matching the values in the second experiment and the final values increasing. As with all of the videos the glare from the lighting has made it difficult to determine the contact point between the two drops.

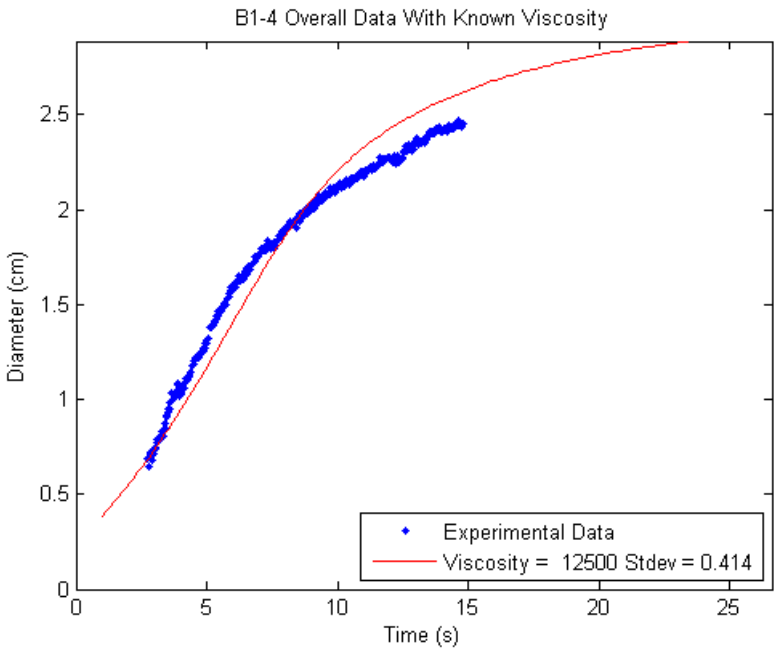


Figure 46: Sample B1-4 with Theoretical Curve for Known Viscosity

Discussion

Two of the videos, B1-2 and B1-4, seemed to have good data sets that correlated with the manufacturer provided value of the viscosity. The other two data sets were inconclusive due to errors introduced by the experimental setup and the method used in the experiment. Droplet size seemed to have an effect on the viscosity measurement for the final portion of the data set, increasing the viscosity measurement with the increase in initial diameter. The initial diameter should have no effect on the measurements and these errors may be due to interference with the stabilizing strings. The viscosity measurement for the initial data did not seem to be affected by the initial diameter. However, there were only two valid measurements for the initial data. More experiments need to be run with known fluids in order to verify this method and accurate viscosity measurements need to be taken prior to running these experiments

in order to determine the accuracy of the measurements for this experiment. However, the two correlating data sets validate the experiment as a feasible method to use after some modifications to the setup.

RECOMMENDATIONS FOR FUTURE WORK

An automated program for performing the analysis was attempted however it was not possible due to three reasons. The first reason is that the black background for the movies with white lines made isolating the droplets from the background nearly impossible for the algorithms provided in the Matlab image processing tool box. The second issue was the lighting. The glare from the lights made it difficult to detect the contact edge of the droplets in both the automated methods and the manual selecting methods that were employed. The glare also contributed to the difficulty in isolating the droplets from the background. The third reason an automated program couldn't be written is because the strings that stabilized and directed the droplets contrasted too much with the background contributing to the difficulty in isolating the drops (Figure 47).

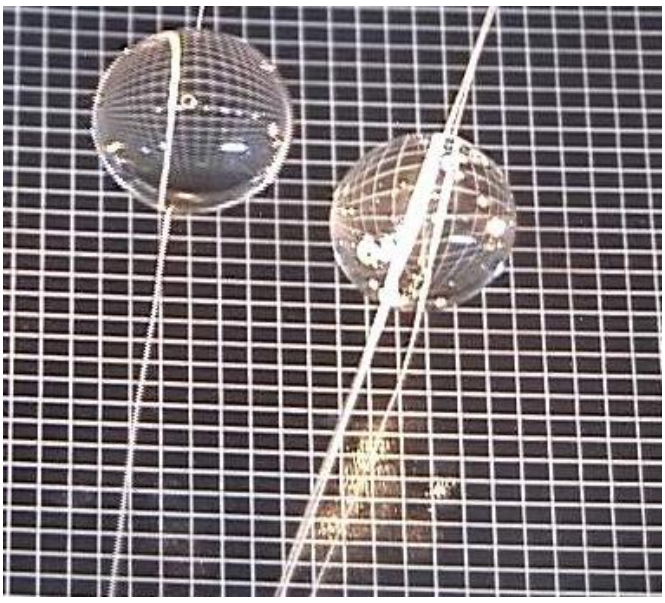


Figure 47: Glair and Support Strings Causing Difficulties in Isolating Drops for Automatic Analysis

There are two recommendations that can be made for future work with these experiments in order to either be able to create an automated program that will determine the contact diameter automatically or to help better find the contact diameter manually. The major reason that the contact diameter could not be determined by the image processing algorithms in Matlab is because of the background. The black background with white lines did not create enough contrast between the background and the drops for the program to be able to isolate the drops. Also the glare from the light created a shifting pattern of contrast on the background which made it too difficult to develop an image filter to remove the background from the image. The string that was used to manipulate the drops also contrasted with the background causing problems for the program and introducing errors in determining viscosity. An easy solution for this issue would be to use a background that was white with lines that are one of the primary video colors, red, green or blue (Figure 48). This color can then be removed from the image leaving only the droplet behind on the image. The string, if still being used, will remain white so that it would blend in to the background. Ground testing should be done so that the program can be developed to analyze the diameter, and so the lighting can be optimized to reduce glare.

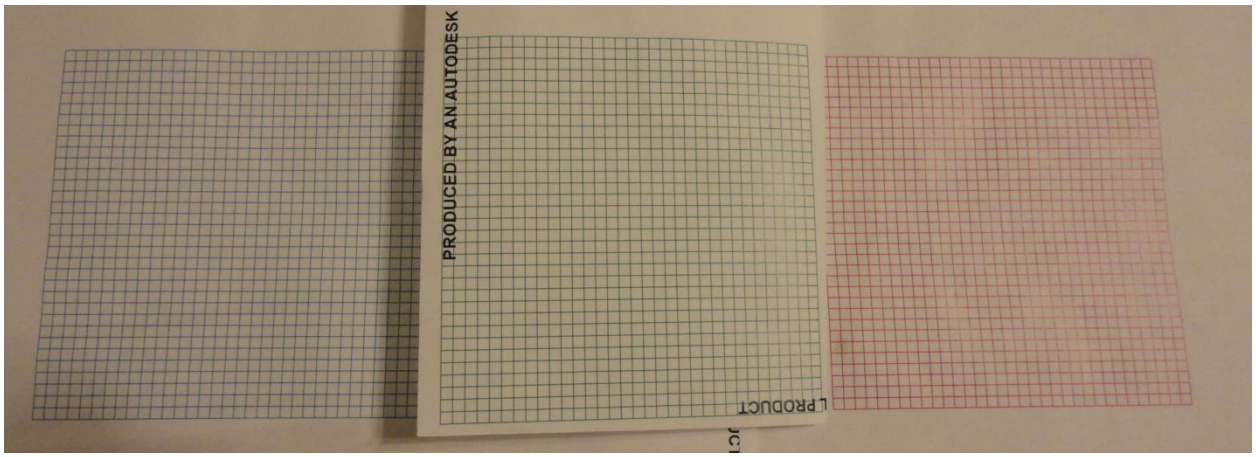


Figure 48: Possible Background Grids for Future Experiments

The second recommendation would be to use a higher resolution camera so that more detail can be seen when determining the contact diameter and will reduce the effects of glare. This will be a must if an automated program is developed and smaller drops are being analyzed.

If this process is to be used in determining the viscosity of under cooled fluids the strings will need to be removed from the setup and the droplets would have to be moved together in some other fashion. If this is to be done the method of moving the droplets together cannot impart a rotational force on the droplets otherwise the assumptions made in the mathematical model for the system will no longer apply

BIBLIOGRAPHY

Antar, B. N., & Nuotio-Antar, V. S. (1993). *Fundamentals of Low Gravity Fluid Dynnamics and Heat Transfer.* Boca Raton, FL: CRC Press.

Antar, B. N., Ethridge, E. C., & Maxwell, D. (2003). Viscosity Mesurment Using Drop Coalescence in Microgravity. *Microgravity Science and Techonolgy , XIV* (1), 9-19.

Dontula, P., Macosko, C. W., & Scriven, L. E. (2005). Origins of concentric cylinders viscometry. *Jurnal of Rheology , 49* (4), 807.

Happel, B. J. (1965). *Low Reynolds Number Hydrodynamics.* Englewood Cliffs, NJ: Prentice Hall.

Ladyzhenskaya, O. A. (1963). *The Mathamatical Theory of Viscous Incompressable Flow.* New York: Gordon & Breach.

Langer, J. (2007, February). The Mysterious Glass Transition. *Physics Today* , pp. 8-9.

Lehman, D. A. (2005). Viscosity Mesurment Technique By Merging Liquid Drops Aboard The International Space Station. Masters Thesis, The University Of Tennessee

Novikov, V. N., & Sokolov, A. P. (2004, October 21). Pissan's ratio and the fragility of glass-forming liquids. *Nature , 431*, pp. 961-963.

Sutterby, J. L. (1973). Falling Sphere Viscometer. *Journal of Physics E: Scientific Instrunments , 6* (10).

Vorst, v. d., & Mattheij. (1995). *Simulation of Viscus Sintering in B E Aplications in Fluid Mechanics.* Southampton and Boston: Computational Mechanics Publications.

White, F. M. (2003). *Fluid Mechanics.* New York, NY: McGraw Hill.

VITA

Brian Godfrey was born in the city of South Bend Indiana to Michael and Joan Godfrey. He was raised in the city until the age of six when he moved to a farmhouse outside of the town of Lakeville Indiana. Through his education and family he was exposed to many activities that would help him later in life such as auto racing and model rocket building. At the age of 19, Brian began a duel degree program where he spent four years studying Physics at Indiana University of South Bend and another two and a half years at Purdue University Calumet studying Mechanical Engineering. In 2008 he received his Bachelor's degree in Mechanical Engineering from Purdue University, and in 2009 he received his Bachelor's degree in Physics from Indiana University. After taking some graduate courses at Purdue University Calumet, Brian applied for and was accepted into the masters program at the University of Tennessee Space Institute. Brian plans on remaining at UTSI and pursuing at PHD in aerospace engineering.